Development of Transfer Standards for SSL Measurement

by

Yiting Zhu

to obtain the degree of Master of Science
at the Delft University of Technology,
to be defended publicly on Monday June 26, 2017 at 10:00 AM.

Student number:	4500350	
Project duration:	October 2, 2016 – July 2, 2017	
Supervisor:	Dr. ir. D. Zhao,	VSL
	Prof. dr. ir. Pavol Bauer,	TU Delft
Thesis committee:	Prof. dr. ir. Pavol Bauer,	TU Delft, supervisor
	Dr. J. Dong,	TU Delft
	Dr. ir. Jose L. Rueda Torres,	TU Delft
	Dr. ir. D. Zhao,	VSL, supervisor

CONTENTS

SUMMARY

SOLID-state lighting (SSL) is the most energy-efficient lighting technology in the present lighting market. With high efficiency, good quality and nice lighting appearance, SSL products are highly expected to replace low efficient and environmental unfriendly incandescent light bulbs in the near future.

An international organization has been established to develop harmonized regulations and global assessment scheme for SSL products. With highly precise measurement setups in test laboratories, the SSL products specifications need to be accurately determined and reliably verified. To fulfill this requirement, a transfer standard is needed to check the reliability of measurement setups in different test laboratories worldwide.

This project aims at developing a transfer standard featured with similar electrical behavior as SSL devices. Key features of the transfer standard are rapid stabilization and switchable configuration to simulate typical SSL topologies.

The electrical characteristics of SSL has been carefully considered in measurement analysis and a complete identification of uncertainty sources in electrical measurement of SSL has been conducted. The transfer standard has been designed by eliminating and reducing the errors from predominant uncertainty sources, such as temperature deviation, power supply voltage fluctuation and instability of the SSL product itself.

Therefore, the transfer standard has been designed into two types of device: the first type is a power electronics converter using a constant-power controller, and the second type is a dummy load device simulating the voltage and current waveforms of SSL products. These two types of transfer standards can both simulate the electrical characteristic of SSL products, achieve rapid stabilization and acquire reliable measurement results. Fluctuations and uncertainties in measurement are minimized.

Compared to the commercial LED lamp, the transfer standard has smaller power variation and shorter stabilization time, which make it applicable to check the reliability of measurement setups as a power reference.

1

INTRODUCTION

1.1. BACKGROUND

LIGHTING uses a lot of energy, representing nearly 20 % of all global electricity use each year [1]. The future development in economy and technology will heavily depend on the capability to light our homes, businesses and streets. Without energy efficiency policies, lighting electricity usage could double by 2030. That means more power plants and more severe environmental issues.

With initiatives to address the global energy crisis, the Energy Independence and Security Act of 2007 demands approximately 25 % greater efficiency for light bulbs, in the time period from 2012 to 2014. In the long term, it also requires roughly 200 % much more efficiency or equivalent energy savings by 2020 [2]. This energy policy significantly prohibits the production and import of most incandescent light bulbs, due to the disadvantages of low efficiency and short lifetimes.

The Alliance to Save Energy Organization supports the Energy Independence and Security Act of 2007 by introducing more energy-efficient LED lights to the lighting market. When compared to traditional light sources, LED technology holds the potential to deliver many benefits, such as lower energy usage, higher quality light, better user control and longer operating life. Although LED prices are much higher than conventional light bulbs, the low energy consumption and longer lifespan can ultimately contribute to lower life-cycle expense.

Nowadays, an increasing number of consumers appreciate the quality and benefits of LED products. However, there are poor-quality LEDs that do not meet consumer expectations. These lamps can burn out prematurely, not produce the promised amount of light or render colors poorly. Dissatisfaction with low-quality LED products from consumers can undermine consumers confidence in LED technology, postpone market penetration and restrict associated energy and environmental benefits.

With the rapid rate of LED development, how governments can promote high-quality LED products that deliver the energy efficiency and other expected benefits to the society has become the most urgency.

1

The International Energy Agency's (IEA) Energy Efficient End-Use Equipment (4E) was launched in July 2010, in which nine countries work together to address global challenges with SSL technologies. Sponsoring governments of the SSL Annex include Australia, Denmark, France, Korea, the Netherlands, Sweden, the United Kingdom and the United States. China also participates as an expert member of the SSL Annex [3].

The Solid-State Lighting (SSL) Annex was established under the framework of the IEA 4E. Realizing the great advantages of international cooperation and joint activities, the SSL Annex works globally to accelerate market adoption of SSL products and promote SSL as an effective way to reduce energy consumption worldwide. With nine member countries, the SSL Annex runs programs focused on LED quality, including assessing and comparing laboratory testing practices around the world, setting performance tools to help governments define quality, exploring the implications of new products features, providing guidance on health and environmental aspects, and identifying best practices in market monitoring verification and enforcement.

For those purposes, the SSL Annex conducted an interlaboratory comparison (IC) program named IC 2013, from October 2012 to August 2013. 110 laboratories have participated in this research, comparing measurements of photometric, colorimetric, and electrical quantities of different types of SSL products [4]. The IC 2013 served as a form of proficiency test (PT) to assess the measurement capabilities for participating test laboratories. The large deviations in measurement results by some laboratories illustrate the importance of PT, since those laboratories will never realize their problems without participating this kind of interlaboratory comparison. Moreover, the interlaboratory differences between worldwide laboratories demonstrate a lot of uncertainty sources in SSL measurement.

The IC 2013 has promoted the mutual recognition of measurement results in SSL products between each test laboratory, lowering technical trade barriers in global lighting market. Knowledge of current state of interlaboratory variation in SSL measurement has also helped determine LED products specifications and promote quality assurance of LED lighting products.

1.2. PROBLEM STATEMENT

EVERY time a new technology is introduced to the market, there are always measurement issues, just as how the current LED market is like.

The most important issue of achieving reliable SSL measurement results is to use highly accurate test setups in laboratories. As a result, a common tool is needed to check the reliability of measurement setups in the proficiency test, which is called the transfer standard.

In previous times, testing laboratories normally use incandescent lamps as transfer standards to prove the reliability of their measurement setups. However, since incandescent lamps will be ousted from the market due to low efficiency, transfer standards based on incandescent lamps will not be used any more. Another limitation of using incandescent lamps as transfer standards is that they are mostly resistive loads, so they are no longer representative for the rising new generation of SSL products.

In the future, testing laboratories have to deal with strongly non-linear, reactive loads containing rich harmonic and inter-harmonic contents in their current waveforms. There-

fore, the newly developed transfer standard should be an electronic load with similar electrical behavior as SSL devices. Key features of the electronic load are rapid stabilization and switchable configuration to simulate typical SSL topologies.

The challenge of using SSL products as electrical test standards is that they are typically not designed to show sufficiently stable electrical behavior due to the temperature-dependent characteristics. For most SSL products, it normally takes about 30 minutes before stabilization, making it difficult to reproduce measurements. In addition, the electrical measurement results of SSL products are in most cases sensitive to environmental temperature and depend on the orientation of mounted lamp.

1.3. METHODS PROPOSITION

THIS project aims at developing an SSL transfer standard lamp used to verify the measurement setups in SSL testing laboratories. This work is funded by the European Union as Joint Research Project (JRP) ENG62 MESaIL, Metrology for Efficient and Safe Innovative Lighting and 15SIB07 PhotoLED, Future photometry based on solid-state lighting products. Additional funding was received from the Dutch Ministry of Economic Affairs.

The transfer standard device is a standard power reference source simulating the feature of SSL products. The design requirements of the transfer standard are listed in the following:

1. Photometric stability of better than 0.1 %;
2. Nearly non-modulated DC-current;
3. Active power (P) controlled within 0.5 %;
4. RMS current (i_{RMS}) controlled within 2 %;
5. Targeting a high power factor (PF);
6. Targeting a low total harmonic distortion of the current ($\mathrm{THD_i}$)

The methods of standard transfer design are proposed in following steps:

1. Investigate the characteristics of SSL products. Compare the differences in operational principles between conventional incandescent lamps and advanced LED lamps, with regard to the transition of transfer standards from incandescent lamps to SSL products;
2. Conduct electrical power measurements using commercial LED lamps. Analyze power fluctuations both in long and short term and perform the uncertainty evaluation of measurements. Among all uncertainty sources, predominant uncertainty sources are identified. For instance, power supply inaccuracy, temperature deviation and instability of the SSL product itself have the most significant influence on the measurement results;
3. Design the transfer standard by eliminating or reducing the errors from predominant uncertainty sources, for example, by using highly accurate power supply, inserting a temperature controller, adopting constant power control scheme and so on;

4. Verify the feasibility of the newly developed transfer standard. Check whether it is able to reach stabilization rapidly and whether the power fluctuation can be restricted to less than 0.1 %.

Based on the design process, there are two potential solutions of the transfer standard LED lamp:

1. A power electronics converter with an optical load (LED)
2. A dummy load with no optical output

Those two types of transfer standards can both simulate the electrical characteristic of SSL products and achieve rapid stabilization. Fluctuations and uncertainties in measurement can be minimized. As a result, designed transfer standards are capable of serving as power reference to check the reliability of measurement setups in worldwide test laboratories for the proficiency test.

REFERENCES

[1] *International energy agency,* .

[2] Wikipedia, *Energy independence and security act of 2007 — wikipedia, the free encyclopedia,* (2017), [Online; accessed 20-February-2017].

[3] *About the 4e solid state lighting annex,* .

[4] *Solid State Lighting Annex: 2013 Interlaboratory Comparison, Final Report*, Energy Efficient End-Use Equipment (4E) International Energy Agency.

2

METROLOGY FOR SOLID-STATE LIGHTING

SOLID-state lighting (SSL) as an energy-efficient newly emerging technology has a promising future. However, market acception is delayed because of inconsistent product qualities and unreliable product performance data. Therefore, an international organization has been established in the aim of promoting harmonized regulations and assessment scheme for SSL products. An interlaboratory comparison has been conducted to show measurement differences and promote mutual recognition between different test laboratories. It also suggests a reliable tool to be designed to check the reliability of measurement setups in test laboratories worldwide.

2.1. CHALLENGES OF SSL METROLOGY

SOLID-state lighting (SSL) is the most energy-efficient lighting technology at the present time. SSL products are normally twice as efficient as fluorescent lamps and ten times more efficient than incandescent lamps [1]. With the potential to reform the efficiency, quality and appearance of lighting, SSL technology is highly expected to replace low-efficient and environmentally-unfriendly light bulbs in the near future. Therefore, scientists are looking for approach to promote SSL technology, in the aim of reducing global electricity consumption and relieving stress on environment.

The most critical problem in promoting SSL technology is the lack of global performance assessment scheme. Without a common test standard, the SSL products specifications cannot be accurately determined or reliably verified. As a result, the quality of products released to the lighting market has a large discrepancy. Poor-quality light bulbs can burn out prematurely, not produce the promised amount of light or render colors poorly, destroying SSL development in the market and damaging consumer confidence in SSL technology.

The challenge of SSL metrology is how to develop harmonized regulations and reliable product certification activities on SSL lighting products. One of the urgency is to

establish the laboratory proficiency test (PT) to check the reliability of measurement setups in test laboratories. Knowledge of the current state of interlaboratory differences in SSL measurements can be derived from interlaboratory comparison. Inconsistency of measurement methods and results should be taken into account in determining products specifications. To address the challenge of SSL metrology, a reliable tool to assess the technical competence of test laboratories needs to be developed.

2.2. HARMONIZATION OF SSL TESTING

LACK of international harmonization of SSL testing leads to difficulties in sharing common measurement methods and exchanging test results. In the situation described in Figure 2.1a, four different regions (USA, Netherlands, China and Japan) independently apply their own test methods and separately conduct proficiency tests. For testers, this kind of independent testing undoubtedly increases workload and expense of each region. No other region accepts the test results from a different region. For manufacturers, they need to obtain accreditation in each region and must pass the proficiency test with each accreditation body for different test methods. Therefore, the situation of expensive and troublesome SSL testing needs to be changed, so that an ideal scheme of global harmonization of SSL testing methods is under development.

Established in 2010, the SSL Annex is an internationally joint organization with an aim of realizing harmonization of worldwide SSL testing. Cooperative governments are Australia, Denmark, France, Korea, the Netherlands, Sweden, the United Kingdom, the United States and China. Those ten countries work together to realize global harmonization as illustrated in Figure 2.1b.

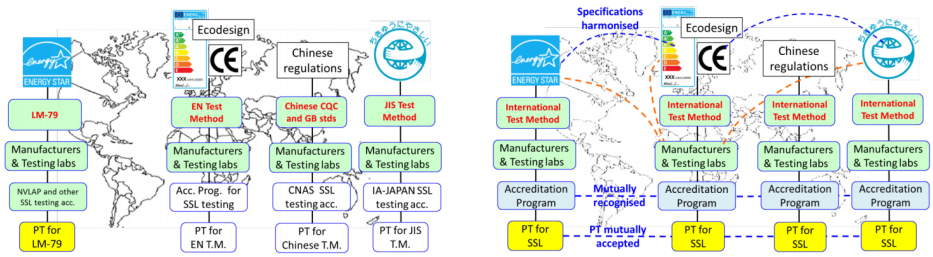

Figure 2.1: The problems associated with harmonization in SSL testing [2]. (a) With poor harmonization of SSL testing, manufacturers need to obtain accreditation in each region and must pass proficiency test with each accreditation body for different test methods. (b) With an ideal harmonization of SSL testing, accreditation programs are mutually recognized and proficiency test are mutually accepted.

In the ideal scheme, test laboratories in different regions apply the same traceable SSL test methods so that the measurement results are reliable enough to be reproduced and exchanged between each region. They conduct common proficiency tests worldwide which can be mutually recognized by each laboratory. With common test methods and proficiency test, four regions are connected with each other, good for government

regulation and market surveillance authorities all around the world.

For the purpose of promoting worldwide mutual recognition of SSL proficiency testing, the SSL Annex's 2013 Interlaboratory Comparison (2013 IC) program involving 110 global SSL test laboratories have been executed. IC 2013 is an interlaboratory comparison of test results from 110 laboratories. The results of IC 2013 can be used as a proficiency test for a participating laboratory that promotes harmonization of SSL testing.

2.3. RESULTS OF PARTICIPANTS MEASUREMENTS

THE IC 2013 was designed to serve as a proficiency test for a participant laboratory. To cover a wide range of participating laboratories worldwide, IC 2013 was conducted by four Nucleus Laboratories including: VSL BV (Dutch Metrology Institute, The Netherlands), National Lighting Test Centre (NLTC, China), National Metrology Institute of Japan - Advanced Industrial Science and Technology (AIST, NMIJ, Japan), and National Institute of Standards and Technology (NIST, USA).

For comparison, five types of lamps were used in IC 2013: incandescent lamps (for reference) and four different LED lamps (directional, omnidirectional, low power factor, and high correlated colour temperature). Participants performed and compared measurements of photometric, colorimetric, and electrical quantities of those five artifacts. Here, only electrical active power is discussed to show measurement differences.

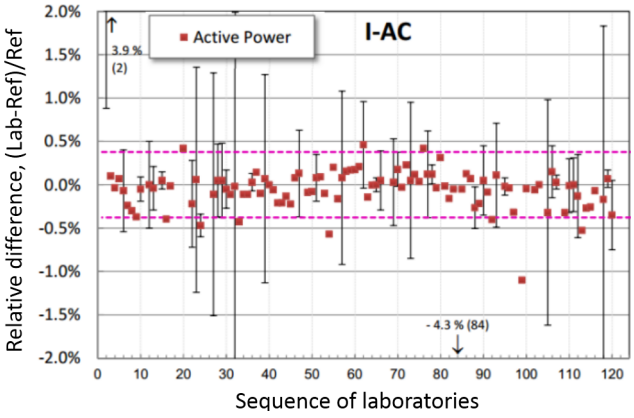

Figure 2.2: Relative differences of active power results for an incandescent lamp measured in 123 laboratories [2]. The horizontal axis represents the sequences of participant laboratories. The vertical axis is relative difference defined as (Lab - Ref)/Ref. Each point indicates a participant laboratory. The dashed pink lines in the figure show the average values of the uncertainties by the reference laboratories for all the points plotted.

It can be observed from Figure 2.2 that points significantly differ with each other, which means various measurement systems can lead to distinguished measurement results. There are even some extremely deviated points in the figures, indicating serious problems in those testing laboratories. The deviation in measurement results from different test laboratories strongly proves the necessity of developing a reliable tool for pro-

ficiency tests.

In the further step, measurement difference caused by variation of lamps is analyzed. Robust standard deviation that minimizes the effects of extreme points is introduced to quantitatively investigate measurement differences among test laboratories. Summary of the relative differences of active power results using robust standard deviation for five different artifact types is illustrated in Figure 2.3.

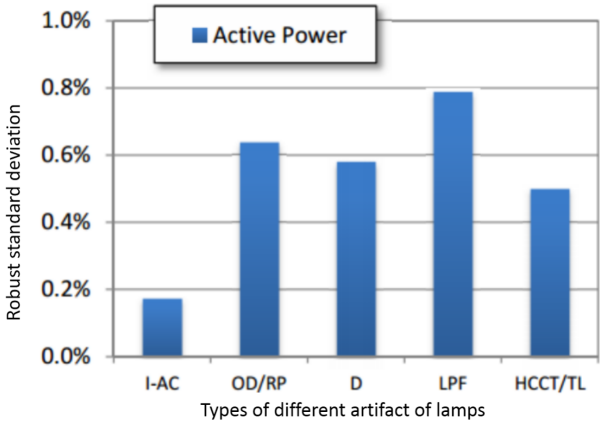

Figure 2.3: Summary of relative differences of active power results for five different artifact types of lamps [2]. The horizontal axis shows five different types of artifact lamps: incandescent lamps (for reference) and four different LED lamps (directional, omnidirectional, low power factor, and high correlated colour temperature). The vertical axis is the robust standard deviation values of five types of lamps. The variations in incandescent lamp measurements are the smallest, less than 0.2 %. In contrast, four LED lamps all have more severe variation, ranging from 0.5 % to 0.8 %, which are on average about 3 to 4 times larger than those of the incandescent lamp.

2.4. DISCUSSION OF MEASUREMENT RESULTS

As a whole, IC 2013 has conducted a global interlaboratory comparison that acts as a proficiency test for SSL products. Measurements of photometric, colorimetric, and electrical quantities were compared using one incandescent lamp and four different types of LED lamps.

It has promoted the mutual recognition of measurement results in SSL products between each test laboratory, lowering technical trade barriers in global lighting market. Knowledge of current state of interlaboratory variation in SSL measurement has also helped determine LED products specifications and promote quality assurance of LED lighting products.

In the results, the large deviation of electrical active power in test laboratories proves that different measurement systems can cause large discrepancy in measurement results. On the other hand, some extremely severe deviations demonstrate the necessity of proficiency testing, since those laboratories would never find out such serious problems in their measurement setups without participating the interlaboratory comparison.

The most important conclusion from IC 2013 is that a reliable tool needs to be designed to check the reliability of measurement setups, which is called the transfer standard. What's more, uncertainty sources in electrical measurement of SSL need to be identified, so that some of the uncertainties can be mitigated to reduce the errors in measurement.

REFERENCES

[1] *Metrology for solid-state lighting,* .

[2] *Solid State Lighting Annex: 2013 Interlaboratory Comparison, Final Report*, Energy Efficient End-Use Equipment (4E) International Energy Agency.

3

UNCERTAINTY ANALYSIS

THE worldwide interlaboratory comparison IC 2013 conducted by 110 testing laboratories presents significant inconsistency in measurement results because each laboratory uses different test methods and test setups. Some measurements even follow out-of-date standards of conventional lighting products, which can no longer fit in SSL testing laboratories. Therefore, in order to acquire reliable measurement results of SSL products, the electrical characteristics of SSL should be carefully considered in measurement analysis. Moreover, a complete identification of uncertainty sources in electrical measurement of SSL is required, so as to eliminate or reduce measurement errors.

3.1. ELECTRICAL CHARACTERISTICS OF SSL

SOLID-state lighting (SSL) products use electroluminescence to emit light, while incandescent lamps use thermal radiation. The greatest difference between SSL products and incandescent lamps lies in that: incandescent lamps are resistive loads with perfectly sinusoidal voltage and current waveforms; while SSL products are highly nonlinear electrical loads with a pure sinusoidal voltage waveform and a non-sinusoidal current waveform. The current waveforms of SSL products are distinguished between each other, depending on the SSL topologies. In uncertainty analysis, five different SSL lamp types are selected for SSL characteristics study, listed in Table 3.1.

Table 3.1: LED lamps used in uncertainty analysis

	Lamp type	Input rectifier stage
L1	4.5 W, 200 lm LED	Simple passive rectifier circuit
L2	12 W, 806 lm LED, dimmable	Active PFC circuit
L3	12 W, 830 lm LED	Unknown
L4	13 W, 810 lm LED	Unknown
L5	7 W, 470 lm LED	Unknown

SSL products as non-linear electrical loads feature non-sinusoidal current waveforms. Different driver topologies of SSL products can generate different shapes of current waveforms. Figure 3.1 shows measurement results of current waveforms of five LED lamps. Current waveform of L1 consists of discontinuous pulses with small time intervals and rather high peak values; while the pulses in current waveforms of L3 and L4 are with wider time intervals and lower peaks.

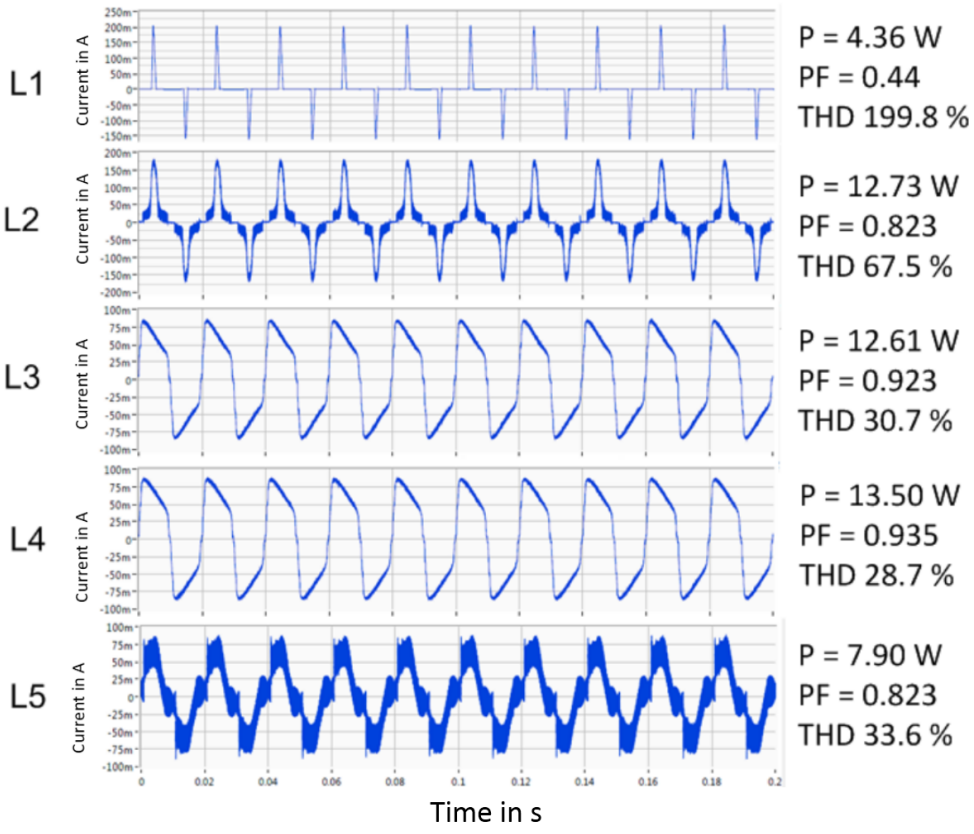

Figure 3.1: Current waveforms of five SSL products. SSL products are featured with non-sinusoidal current waveforms due to nonlinearity. The current waveforms are different between each lamp depending on their driver topologies. L1 shows the most distorted current waveforms, the lowest power factor (PF) and the highest total harmonic distortion (THD) in current because of no power factor correction (PFC) circuit in its driver topology.

Based on different driver topologies of SSL products, the current waveforms can be classified into two types with regard to harmonics performance: SSL products with rich current harmonics in low frequency and with rich current harmonics in high frequency.

3.1.1. RICH CURRENT HARMONICS IN LOW FREQUENCY

For SSL lamps featuring driver topologies with no power factor correction (PFC) circuit, their current waveforms are seriously distorted. As shown in current measurement results of L1 in Figure 3.1, the current extracted from the power supply is consisted of discontinuous pulses with narrow time intervals and rather high peak values.

The reason is that in SSL driver topologies the input side usually involves a rectifier circuit following a storage capacitor that operates in keeping a voltage approximately around the peak value of input wave until the next peak arrives to refill the capacitor. Therefore, current only flows near the peaks of the input waveform, appearing as several pulses. Every current pulse contains large energy to sustain the load until the next peak, by charging the capacitor a pulsed time and then discharging the stored energy to the load for the rest time in the cycle. Commonly, the current pulse can be 10 % to 20 % of the cycle, which means the pulse carries 5 to 10 times the average current.

Current crest factor is very high in such SSL lamps without PFC circuit, which is defined as the ratio of waveform's peak value to its rms value. For sinusoidal waves, current crest factor is 1.414. For non-sinusoidal waves as current of L1, current creast factor is higher, about 4.22.

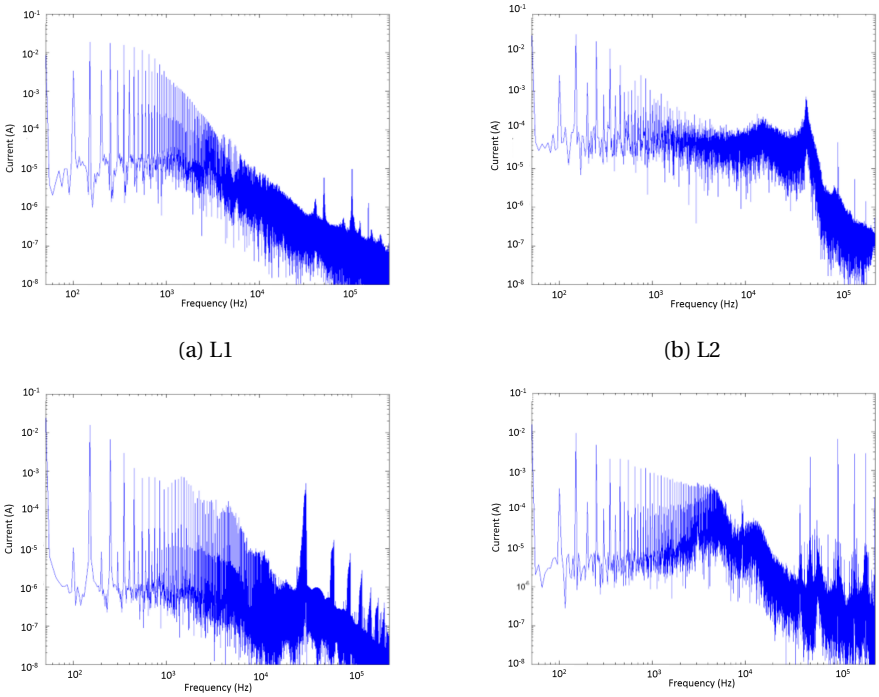

(a) L1 (b) L2

(c) L3/L4 (d) L5

Figure 3.2: Current spectrum shows rich current harmonics in SSL lamps. The horizontal axis is the frequency and the vertical axis is the amplitude of current at certain frequency. L1 has rich current harmonics in low frequencies, while other lamps have rich current harmonics in high frequencies

Current waveforms of such SSL lamps have rich current harmonics in the low-frequency range from 100 Hz to 2 kHz. The current harmonics are low in high frequencies. Figure 3.2a is the current spectrum of L1 which has rich low-frequency harmonics. In low-frequency region, current level is relatively high and the slope of asymptote is about 0 dB/decade; while in high-frequency region, current level is much lower and decays rapidly with frequency.

3.1.2. RICH CURRENT HARMONICS IN HIGH FREQUENCY

For SSL driver topologies with PFC, the current waveforms are refined to match the shape of the sinusoidal voltage waveforms. As shown in current waveforms of L2 in Figure 3.1, the pulses have wider time intervals and lower peaks than those of L1. Compared to such SSL without PFC, the power factor is improved from 0.44 to 0.823 and total harmonic distortion (THD) is reduced from 199.8 % to 67.5 %.

Such SSL lamps have rich current harmonics in the high-frequency range above 2 kHz. Figure 3.2b shows the current spectrum of SSL lamps with rich high-frequency harmonics. In low-frequency area, the slope of asymptote is about -20 dB/decade so that the low-frequency current harmonics rapidly decay to a low level; while in high-frequency region, the current harmonics always keep at a high level and the peak current value appears around 40 kHz. L3, L4 and L5 have similar harmonic characteristics.

3.2. MEASUREMENT RESULTS

TWO scenarios are constructed to figure out the uncertainty sources from measurement setups and test conditions. The first scenario is called standard scenario, in which the measurements are conducted under publicly available power meters, which is relatively low quality; the second scenario is called stringent scenario, in which the measurements are carried out by equipment with high resolution, high sampling rate digitizer, and advanced algorithms. The detailed description is illustrated in Figure 3.3.

Item		Standard scenario	Stringent scenario
1	Meter	Commercially available power meter/ analyzer	24-bit resolution, sampling frequency 500 kSa s^{-1} digitizer, 100 kSa each measurement
2	Transducer	12-bit resolution, Sampling frequency 100 kSa s^{-1}	Wide-band (>20 kHz) voltage divider Wide-band (>100 kHz) current shunt
3	Algorithm	Bandwidth 50 kHz	Integration and FFT approaches. Interharmonics are considered.
4	AC power supply	$THD_u < 3\%$	$THD_u < 0.5\%$
5	Ambient condition	±1.0 °C	±0.5 °C
6	Stabilization of each measurement	At least 3 readings of the electrical power over a period of 30 min, taken 15 min apart, is less than 0.5%	At least 3 readings of the electrical power over a period of 30 min, taken 15 min apart, is less than 0.2%
7	Voltage regulated	±0.2%	±0.1%
8	Connection	Not defined	The connections between the power supply, transducer and lamps are kept as short as possible

Figure 3.3: Comparison of standard scenario and stringent scenario. The stabilization of each measurement should be less than 0.5 % for standard scenario and less than 0.2 % for stringent scenario.

Apart from measurement setups and test conditions, lamp types also affect the mea-

surement uncertainties. Therefore, measurement and uncertainty analysis should be done for different SSL lamps. Five lamp types are chosen to do comparison, as previously described in Table 3.1. Based on the analysis in Section 3.1, L1 has a simple passive rectifier circuit with no PFC and it has rich current harmonics in low frequency. In contrast, L2 has a PFC circuit at the input side so that its current harmonics are rich in high frequency. L3, L4 and L5 have similar harmonic characteristics as L2, except that L5 shows capacitive reactance in the input stage.

The electrical specifications including active power P and RMS value of current I_{RMS} are mainly discussed, since P is directly measured by test setups and most required, and I_{RMS} is relevant to power factor of lamps.

Electrical measurement results of five SSL lamps under the stringent scenario and standard scenario are illustrated below in Table 3.2.

Table 3.2: Relative differences in two scenarios

	Standard	Stringent
P	2 %	0.6 %
I_{RMS}	6 %	3 %

Measurement results show that relative differences of both active power P and RMS value of current I_{RMS} are smaller in stringent scenario than in standard scenario. Therefore, higher quality test setups and better regulated test environment can reduce measurement uncertainties and contribute to more accurate results. In the following section, uncertainty sources are figured out based on the difference between standard and stringent scenario construction.

3.3. UNCERTAINTIES ANALYSIS

THIS section discussed about the measurement uncertainties due to the measurement equipment, the test conditions and the interaction between them.

3.3.1. MEASUREMENT EQUIPMENT

Uncertainties in power and current due to the measurement equipment can be eliminated by refining devices, for example using a power meter with wider bandwidth and higher accuracy.

ERROR DUE TO WIRING METHOD

The wiring method of the power meter can influence measurement results of voltage, current and power. Selecting a proper wiring method can improve accuracy in SSL measurement. There are two wiring methods commonly used in SSL power measurement, as shown in Figure 3.4.

In Figure 3.4a, the voltage meter is directly connected across the lamp. By this way, the large voltage across the current meter will have no effect on the voltage meter value.

In Figure 3.4b, the current meter only measures the current flowing through the lamp, so that the current through the voltage meter has no disturbance on the current measurement.

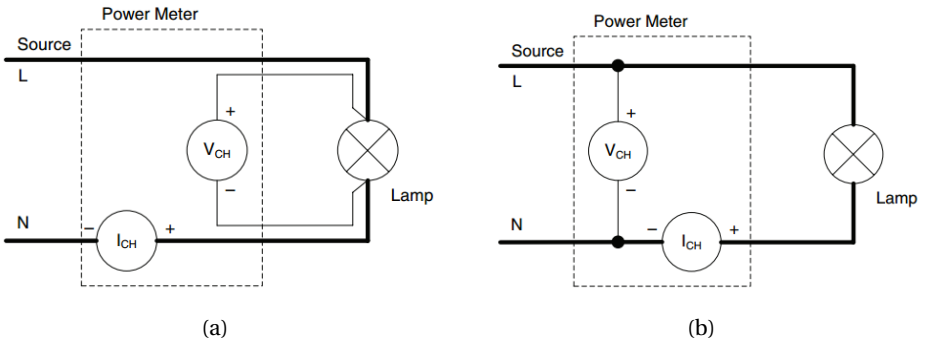

Figure 3.4: Wiring of the power meter in power measurement [1]. (a) When the power meter impedance is large enough, the lamp impedance can be neglected. The current flowing through the voltage meter can also be neglected, so the current meter only measures the current through the lamp, and the voltage meter makes no error on the current measurement. (b) The wiring is applied When the current flowing through the lamp is low enough so that the voltage drop on the lamp can be neglected.

ERROR DUE TO LIMITED BANDWIDTH

Each power meter has a limited bandwidth, and its frequency response goes down at high frequencies, as shown in the red line in Figure 3.5. The relationship between the bandwidth of the power meter and SSL products has an influence on the measurement results.

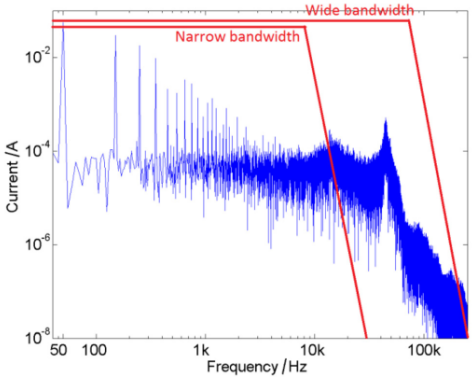

Figure 3.5: Frequency responses of the LED lamp L2 and the power meter. If the bandwidth of the power meter is wider than the highest frequency of current harmonics, it is able to measure all components of current harmonics in high frequencies. Otherwise, the power meter cannot measure the high-frequency components in current waveforms.

For SSL products with rich current harmonics at high frequency, if the bandwidth of power meter is too narrow, the high-frequency part of current harmonics can not be measured by the power meter. In the frequency response of L2 (in blue) in Figure 3.5, there are rich current harmonics at high frequencies and the peak current shows up at

around 40 kHz. Current can be completely measured only if the power meter bandwidth (in red) is wide enough, including all high-frequency current.

3.3.2. TEST CONDITIONS

The uncertainties in power and current caused by the test conditions can be eliminated via using stringent test conditions, for example a stable temperature environment and a precisely regulated voltage supply.

ERROR DUE TO TEMPERATURE DEVIATION

The electrical active power measurement of SSL products strongly relies on temperature because of the temperature effect on IV characteristic of diodes. When the temperature rises as the LED lamp emits light, its IV curve shifts to the left side. Depending on different control schemes, the LED operating point changes with the temperature and causes power variation.

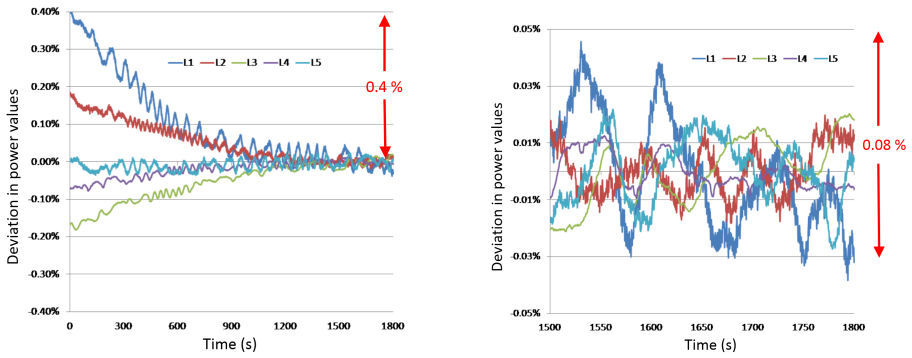

(a) (b)

Figure 3.6: Variation of power values before stabilization. Active power of 5 LED lamps is measured every 0.2 s. The horizontal axis is the time in seconds and the vertical axis is the deviation in power values in percent. (a) Power variation 30 minutes before stabilization. The greatest power deviation is about 0.4 % in L1. (b) Power variation 5 minutes before stabilization. There are still small ripples in power values due to the instability of the LED lamps themselves.The maximum power deviation is about 0.08 % for L1.

In Figure 3.6a, active power of 5 LED lamps is measured every 0.2 s during the last 30 minutes before stabilization. The long process before stabilization ends until the lamps achieve thermal balance. 5 curves of measured power can be going up and down, depending on the control scheme of each lamp circuit.

If the LED topology is under constant-current control, when the temperature rises the converter regulates the output current at a constant level and reduces the voltage drop across LED loads. Due to constant current and reduced voltage, the measured power goes down with rising temperature. The curve of L1 and L2 drops from the beginning and goes stable after about 30 minutes.

Similarly, if the LED topology is under constant-voltage control, when the temperature rises the converter regulates the output voltage at a constant level and increases the current flowing through LED loads. Due to constant voltage and increased current, the measured power goes up with rising temperature, shown as the curve of L4 and L5 in Figure 3.6a.

L3 is under power-constant control scheme. As the IV curve shifts, the circuit regulates both current and voltage at the same time so that their product is kept at a constant value. So the power measurement is not influenced by temperature. The curve of L3 keeps at a stable level from beginning to end.

30 minutes before stabilization is a rather long process in measurement so that the results are not reproducible. The deviation of power before stabilization can be up to 0.4 %. As a result, the errors in power measurement should be eliminated by keeping temperature at a stable level.

ERROR DUE TO THE SSL PRODUCT

Figure 3.6b records the measured power of 5 LED lamps five minutes before stabilization. Even though measured power has already reaches a relatively stable level, there are still small ripples after stabilization. It is observed that the power fluctuation can be 0.05 %. Depending on different types of SSL products, the power variation differ between each other and L1 fluctuates most.

ERROR DUE TO POWER SUPPLY VOLTAGE REGULATION

Uncertainties in current measurement are estimated as the same order of the deviation of supply voltage, so the fluctuation of supply voltage affects measurement results. To reduce uncertainties due to power supply, AC voltage should be kept within ±0.2 %. Using a highly precise power supply could be a solution to improve measurement accuracy.

3.3.3. INTERACTION BETWEEN THE MEASUREMENT SETUP AND THE DUT

Uncertainties due to the the interaction between the measurement setup and the device under test (DUT) can be eliminated by improving measurement setups to minimize the interaction, such as using a shunt resistor with lower resistance and applying a impedance stabilization network to suppress high-frequency resonance.

ERROR DUE TO THE SHUNT RESISTOR

There is a shunt resistor in the power meter that converts the current into voltage. Shunt resistances can differ from mΩ to Ω, leading to large changes in current waveforms.

Three laboratories use three different shunt resistors in measurement and achieve different results on currents. The current measurement results with the change of frequencies are shown in Figure 3.7.To reduce the influence of the shunt resistor to current measurement, the resistance should be restricted under 0.2 Ω.

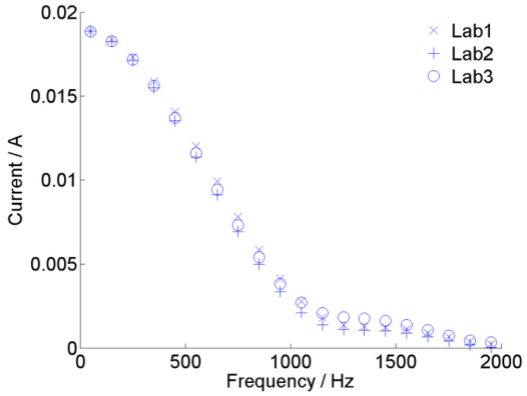

Figure 3.7: Influence of shunt resistors on current measurement results. Lab 1, Lab 2 and Lab 3 apply power meters with different shunt resistors. The greatest difference between three results happens at around 900Hz, the resonant frequency of the 4.7 mH inductor and the 6.8 μF capacitor in L1 circuit.

ERROR DUE TO THE POWER SUPPLY IMPEDANCE

For LED lamps with a capacitive input rectifier such as the L5 lamp, the resonance happens in the whole measurement system can be a significant source of uncertainties. The frequency and amplitude of the high-frequency resonance are depend on the inductive reactance of the cable and the power supply, explaining measurement differences among laboratories.

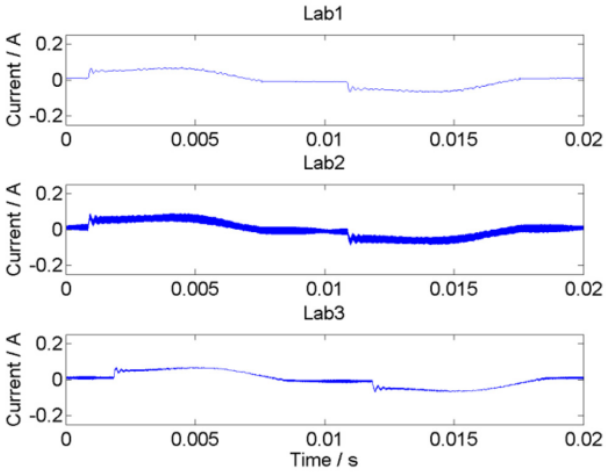

Figure 3.8: Current measurement results from three labs show the occurrence of high-frequency resonance. Lab 1, Lab 2 and Lab 3 apply power meters with different power supply. The width of the current waveforms is actually the amplitudes of oscillations due to high-frequency resonance. Results from Lab2 have the most severe resonance.

In Figure 3.8, the width of the current waveforms is actually the amplitudes of oscillations due to high-frequency resonance.

3.4. DISCUSSION AND CONCLUSIONS

FOR the active power measurement, the predominant uncertainty sources are temperature deviation, power supply voltage fluctuation and instability of the SSL product itself. For the RMS current measurement, limited bandwidth, shunt resistance and power supply source impedance significantly affects results.

Some uncertainties can be overcome by applying stringent scenarios such as using an accurate power meter and a precisely regulated power supply. However, other errors which come from the temperature variation and SSL products themselves can not be eliminated in real measurement environment.

Such unavoidable uncertainty sources make measurement results from different test laboratories not reproducible or reliable. Each laboratory applies different measurement setups and test conditions that causes large uncertainty and discrepancy in measurement results. Different types of lamps used for measurement also lead to inconsistency in measurement.

As a result, the transfer standard used to check the reliability of measurement setups in test laboratories should be able to resist the uncertainties from measurement setups and test conditions, especially temperature deviation and power supply fluctuation. In the same word, the transfer standard should be a constant power electrical load so that the power meter can acquire accurate measurement results in a short time. No matter how the temperature changes in test laboratories or no matter how the setups differ between laboratories, measurement setups can be validated by reliable results with the help of the transfer standard.

REFERENCES

[1] D. Zhao, G. Rietveld, J.-P. Braun, F. Overney, T. Lippert, and A. Christensen, *Traceable measurements of the electrical parameters of solid-state lighting products,* Metrologia **53**, 1384 (2016).

4

TRANSFER STANDARD CRITERIA DESIGN

TRANSFER standard LED lamp is designed to rapidly reach a constant level of electrical active power to minimize measurement duration, and its power fluctuation should be kept rather low to ensure the measurement results reproducible. Since the existing LED lamps in lighting market are mostly under constant-current control, they can not meet the requirements of constant power for test laboratories. As a result, a new LED lamp using constant-power control that can be especially served as a transfer standard is designed in this project.

4.1. LED DRIVER

FIGURE 4.1 shows a typical LED system comprising of an AC power supply mains, an LED driver involving feedback or control signals, and several LED lamps. The LED driver, also called the LED power supply, is the most important part in an LED system, ensuring normal function and best performance of LEDs. If the LEDs are not sufficiently supplied with power, its light flickers or is considered as choppy, making LED lamps non-ideal light sources and thus damaging consumers confidence in LED technology.

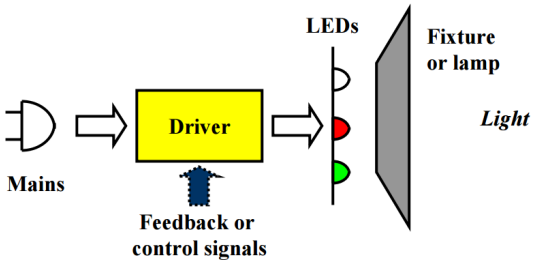

Figure 4.1: Configuration of a typical LED system [1]. An LED system includes AC power supply mains, an LED driver involving feedback or control signals, and several LED lamps.

LEDs need special drivers for two main reasons:

1. An individual LED for illumination requires 2-4 *V* DC voltage and several hundred mA DC current. Since LEDs are usually connected in series in an array, 12-24 *V* DC voltage is required. However, LEDs are normally supplied by high AC voltage about 120-277 *V* and alternating current. Therefore, LED drivers should be able to rectify high AC voltage and alternating current to low DC voltage and direct current.

2. LEDs drivers should prevent LEDs from voltage or current variations, which means provide a constant-voltage or constant-current output control. Since LED light output is directly proportional to its current output, keeping a constant current level can ensure a stable light output so as to make human eyes comfortable. Current fluctuation leads to light variation or degradation that undermines the quality of LED products.

In conclusion, LED drivers act as power supplies for LED systems. They convert high AC voltage and alternating current to low DC voltage and direct current, and regulate the voltage and current across LED at rated levels.

4.2. LED DRIVER CONTROL SCHEME

IN LED technology, LED driver design is the most difficult part. There are a lot of different types of LED drivers available in the market, designed for realizing various electrical requirements in lighting application.

Many factors are to be considered in choosing an LED driver, for example optical factors such as light intensity, color and brightness. There are also other elements that make sense, like operating temperature, environmental consideration and budget plan.

For electrical design, choosing a constant-current or constant-voltage LED driver is a main concern. Pros and cons of each control scheme will be illustrated in the following.

4.2.1. CONSTANT-CURRENT DRIVERS

The constant-current drivers shown in Figure 4.2 is able to deliver constant current flowing through LEDs across a defined output voltage range. Since multiple LEDs are normally connected in series, constant-current drivers can make sure a stable level of luminous intensity and chromaticity from each LED after thermal stablization.

One unique characteristics of LED is the exponential relationship between the applied forward voltage and the resulting current flowing through it. Refer to the I-V curve of Cree XP-G2 LEDs shown in Figure 4.3, when the LED is switched on, a rather small 3.5 % deviation on the voltage source (from 2.75 V to 2.85 V) can lead to a 100 % difference (from 250 mA to 500 mA) in the forward current.

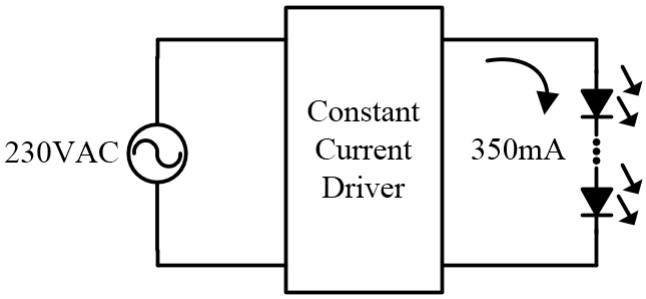

Figure 4.2: Constant-current LED driver circuit. The current output of the current-regulated LED circuit is 350 mA. Several LEDs are wired in series to provide required luminous flux.

Although higher forward current can generate brighter light on the LED, it may also over-drive the LED. Figure 4.4 specifies Cree XP-G2 LEDs maximum forward current and de-rating curves in different ambient temperature conditions. The maximum forward current is determined by the ambient temperature and the thermal resistance between the LED junction and ambiance. Higher the temperature, lower the maximum forward current the LED can withstand.

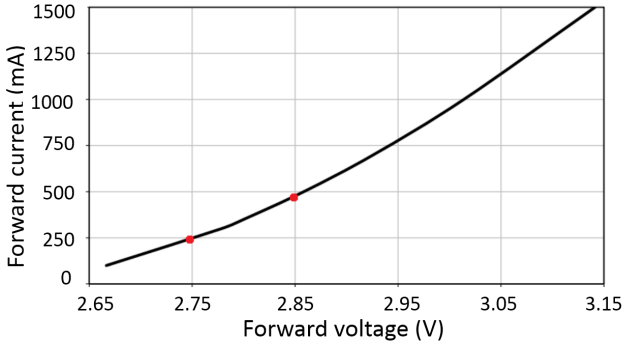

Figure 4.3: I-V characteristics of XP-G2 LEDs [2]. A rather small 3.5 % deviation on the voltage source (from 2.75 V to 2.85 V) can lead to a 100 % difference (from 250 mA to 500 mA) in the forward current.

Based on the example of XP-G2 LEDs mentioned before, the 3.5 % small voltage deviation causing 100 % current difference is able to push the forward current to exceed the limitation at a higher ambient temperature. The excessive forward current will generate extra heat in the system, cut down on the LEDs lifespan, and finally damage the LED.

Therefore, constant-current drivers are preferred to regulate the current and prevent LEDs from exceeding absolute maximum current rating for reliability. Small thermal resistance and low ambient temperature are preferred for long lifetime and optimized

optical characteristics.

In conclusion, constant-current LED drivers the most popular in LED driver application. The advantages of using constant-current LED drivers are that:

1. To avoid violating the Absolute Maximum Current Rating specified for LEDs, therefore preventing failure caused by heat.

2. To generate predictable and matched luminous intensity and chromaticity from each LED.

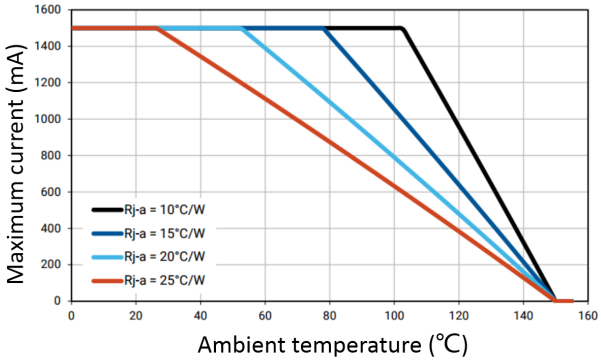

Figure 4.4: Cree XP-G2 LEDs maximum forward current and de-rating curves in different ambient temperature conditions [2]. The maximum current is determined by the ambient temperature and the thermal resistance between the LED junction and ambiance. Higher the ambient temperature and larger the thermal resistance, lower the maximum forward current the LED can withstand.

4.2.2. CONSTANT-VOLTAGE DRIVERS

The constant-voltage driver shown in Figure 4.5 delivers fixed output voltage to loads, typically 12 VDC or 24 VDC. In real application, a group of LEDs are commonly connected in both series and parallel to generate desired light intensity or color. The current-limiting resistor is added to keep a constant current through each LED string in the constant-voltage output. However, the power consumption in the current-limiting resistor reduces efficiency of constant-voltage circuits.

The advantages of constant-voltage LED drivers are that:

1. They have more flexibility to connect incremental LED strings up to the maximum power rating, suitable for situations when the number of LED loads is unknown prior to installation.

2. Design engineers and installation technicians tend to be more familiar with the constant-voltage technology and it normally cost less.

The disadvantages of using constant-voltage LED drivers are that:

1. Tend to violate the maximum current specified for LEDs as temperature increases.

2. Current-limiting resistors add complexity and reduce energy efficiency of the circuit.

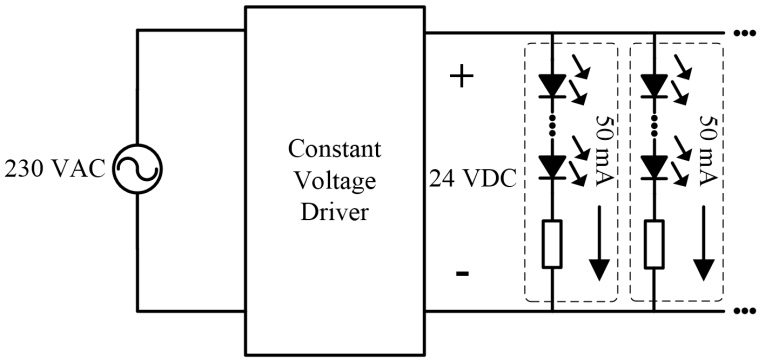

Figure 4.5: Constant-voltage LED driver circuit. The fixed output voltage is 24 VDC. LEDs are connected in series with a current-limiting resistor, and then several LED strings are paralleled to each other receiving the same voltage.

4.3. OTHER FACTORS CONSIDERATION

SINCE the LED driver is the most important part in an LED system, many factors should be included in choosing a proper driver. Performance of regulated output, power factor correction and efficiency is the first priority, and environmental concerns such as temperature range, lifetime and safety also make sense. This section explains some other factors to be considered in choosing an LED driver.

4.3.1. POWER FACTOR

Power factor (PF) is an important consideration for a power supply, since it describes how efficiently an LED driver can make use of electricity. It is expressed into the power being used by the driver divided by the product of the input voltage times the input current. The range of power factor is a decimal between 0 and 1. The closer to unity, the more efficient the driver is. The LED driver is expected to have a power factor of about 0.9 or above.

LED drivers datasheets also introduce a term of total harmonic distortion (THD). In electrical devices with non-linear loads, THD is an important factor because the distortion of the sinusoidal waveform can cause potentially dangerous consequences, such as the overheating of electrical equipment and even fires in transformers and switching stations. THD below 20 % is usually acceptable and a THD of less than 10 % is exceptionally good.

4.3.2. LIFETIME

Driver lifetime is another major concern. The LED lifetime greatly drops down with increasing temperature. On the label of most LED drivers there is a small circle called the hotspot, which is usually the hottest point used to determine the temperature. If the

driver is used close to this limiting temperature, its operating lifetime will be shorter than if operated at a lower temperature.

4.3.3. DIMMING

Dimming means lowering the brightness of a light by adjusting the voltage waveform applied across the LED. A 10 % dimming is able to save 90 % of energy consumption, that is helpful to energy conservation. However, only dimming down below 1 % can be recognized by human eyes, so drivers capable of dimming down below 1 % are needed for a dimly-lit room or theater and down to 0.1 % for full-range dimming.

4.4. TRANSFER STANDARD DRIVER DESIGN

THE transfer standard LED lamp design requires that it can rapidly reach a constant level of electrical active power to minimize measurement duration, and keep power fluctuation low enough to make reproducible measurement results.

Since the existing LED lamps in lighting market are mostly constant-current or constant-voltage, they can not meet the requirements of constant power for test laboratories.

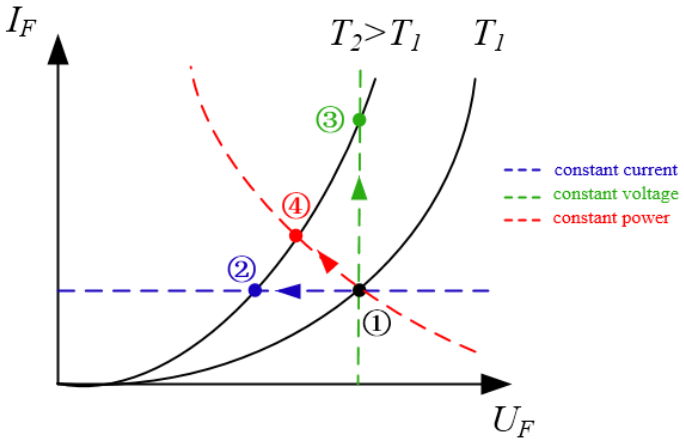

Figure 4.6: Three control schemes of LED driver design: constant current, constant voltage and constant power. The initial operating point is ①. Under the constant-current control (in blue), the operating point changes from ① to ③, so the voltage drops and the power decreases. Under the constant-voltage control (in green), the operating point changes from ① to ③, so the current goes up and the power increases. Under the constant-power control (in red), the operating point changes from ① to ④, so that the voltage drop can be offset by the current rising.

When the temperature rises, the LED I-V curve shifts to the left side, as shown in Figure 4.6. Under constant-current regulation drawn in the blue line, the driver regulates the output current at a constant level and reduces the voltage drop across LED loads, with the operating point shifting from ① to ②. Due to constant current and reduced voltage, the measured power goes down with rising temperature.

Under constant-voltage regulation drawn in the green line, when the temperature

rises the driver regulates the output voltage at a constant level and increases the current flowing through LED loads, with the operating point shifting from ① to ③. Due to constant voltage and increased current, the measured power goes up with rising temperature until thermal stabilization reaches, and it normally takes longer than 30 minutes.

As a result, a new LED lamp using constant-power regulation that can be especially served as a transfer standard should be designed. When the I-V curve shifts with temperature deviation, the circuit regulates both current and voltage so that their product is kept at a constant value, with the operating point shifting from ① to ④ as shown in the red line.

REFERENCES

[1] Philips-Advance, *Led drivers-a practical understanding of lighting application,* .

[2] T. Scully, *What type of led driver do i need? constant current vs. constant voltage,* .

5

TRANSFER STANDARD CONTROL DESIGN

UNTIL now, the transfer standard driver has been defined to be a constant-power regulator. In the next step, the driver control scheme will be designed, for example, primary or secondary side regulation, feedback or feedforward control, in consideration of reliable control and simple topology.

5.1. PRIMARY AND SECONDARY SIDE REGULATION

FLYBACK converter is commonly applied in low-power situations especially in LED drivers because of its simplicity and cost efficiency. It uses a transformer for energy storage and isolation between mains and loads. In most LED applications, constant current regulation is needed for luminous stability and reliable operation. The most popular method is to sense the output current at the secondary side and feed it back to the primary side using an opto-coupler. Since the opto-coupler has power dissipation and adds components to the circuit, other control schemes needs to be developed for higher efficiency and simpler topology.

5.1.1. SECONDARY SIDE REGULATION

In conventional flyback converters, output voltage regulation and output current regulation are realized by an opto-coupler and an error amplifier feedback loop. The opto-coupler converts optical signal at the secondary to electrical signal that controls the switch duty cycle, and at the same time keeps an isolation barrier. This kind of secondary side regulators directly measure output voltage and current so that they can accurately control the output results, but at the cost of complexity. Figure 5.1 shows a typical secondary side regulator using opto-coupler.

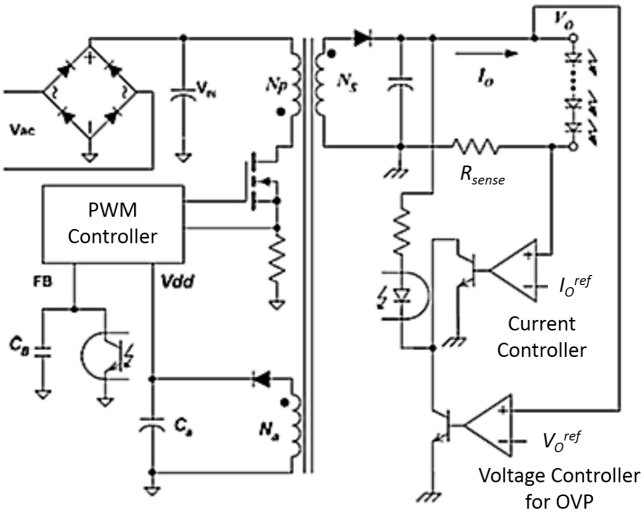

Figure 5.1: A secondary side regulator using opto-coupler [1]. The actual output current I_o is measured by a sense resistor R_{sense}, then sent to a current controller and compared to a reference value I_o^{ref}, generating an error signal. In the same way, the actual output voltage V_o is measured, sent to a voltage controller and compared to a reference value V_o^{ref}. Afterwards, the error is transmitted to the primary side using an opto-coupler. The PWM controller receives signals from opto-coupler and sends the gate signal to the switch so that the output current and voltage can be tightly controlled.

Although the opto-coupler provides a straightforward way to acquire the information of the output results, the secondary side regulation including an opto-coupler has several disadvantages listed below:

1. Opto-coupler's transfer ratio is not stable because it changes with temperature deviation and its propagation delay can affect the dynamic response of the control loop. Opto-coupler also degrades over time.
2. The secondary side regulation, involving an opto-coupler, reference voltage and a sense resistor, adds a large number of components at the secondary side. The complicated topology and redundant components cause difficulties in PCB design.
3. The feedback loop requires more components and consumes extra power, so it increases system expense and decreases efficiency.

For those disadvantages of secondary side regulation, a non-opto-coupler option should be considered to improve the output regulation and to simplify the topology.

5.1.2. PRIMARY SIDE REGULATION

In contrast to secondary side regulation, primary side regulators (PSR) do not directly sense the output voltage or current information. Instead, they infer output performance by using primary information. Without the opto-coupler and feedback loop from secondary side, the converter becomes simpler and smaller and thus much cheaper.

The most important point of primary side regulation is how to acquire the output voltage and current information without actually sensing or measuring them. If the information can be obtained by indirect ways, it will be simple to use the conventional feedback loop to control the output parameters.

For example, a primary side regulated flyback converter that can realize constant voltage and constant current has been proposed in [2]. This PSR circuit directly uses the voltage signal received from the auxiliary winding at the primary side to control the switch duty cycle, so as to stabilize the output current and voltage applied on the load. Figure 5.2 shows its circuit diagram and typical waveforms.

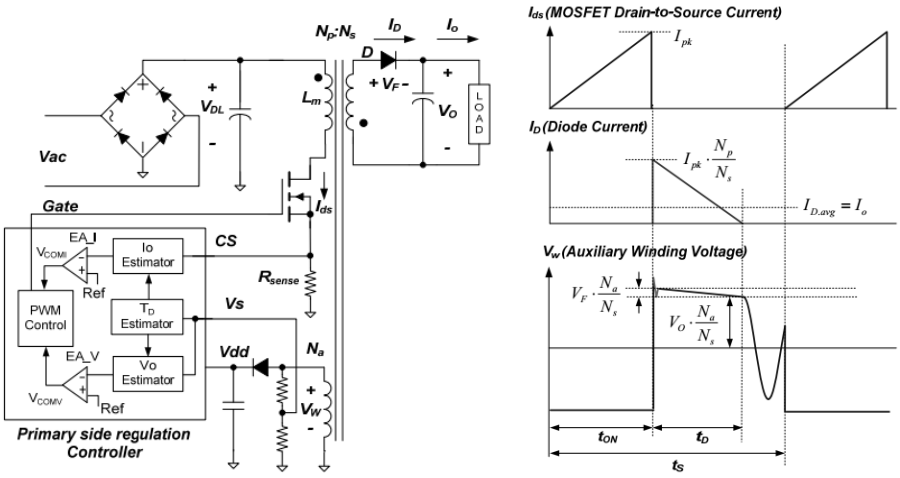

Figure 5.2: Topology and key waveforms of a primary-side regulated flyback converter [2]. The primary current I_{ds} rises when the switch is on and the diode current I_D drops down when the switch is off. The voltage across the auxiliary winding V_W reflects the output voltage information.

In a switching period, there are three operational modes:

1. In t_{ON} when the MOSFET is on , the rectified voltage V_{DL} from the AC input is applied to the primary inductor L_m. The energy is extracted from the input and stored in the inductor. So the MOSFET current I_{ds} rises linearly from zero to the peak value I_{pk}. No current flows through the secondary side.

2. In t_{D} when the MOSFET is off, the energy previously stored in the core generates current flowing though the diode D at the secondary side. During the diode conduction time t_D, the voltage across the secondary inductor is the sum of output voltage V_o and diode forward-voltage drop V_F. The diode current I_D drops lin-

early from maximum $I_{\text{pk}} \cdot N_p / N_s$ to zero in the end, which also means all energy in the inductor has been completely released to the load.

3. In the remaining time $t_{\text{s}} - t_{\text{ON}} - t_{\text{D}}$, the auxiliary winding voltage V_w starts to oscillate because of the LC resonance between the primary-side inductor and the MOSFET output capacitor.

For constant-voltage regulation, the output voltage information can be obtained by sampling the voltage across the auxiliary winding at the primary side.

In diode conduction time t_{D}, the secondary winding voltage is $(V_o + V_F)$, the sum of output voltage and diode forward voltage. This voltage is transformed to the primary auxiliary winding side as $(V_o + V_F) \cdot N_a / N_s$. The diode forward voltage decreases from V_F to zero when the diode current decreases from its peak value to zero. So the auxiliary winding voltage V_w decreases from $(V_o + V_F) \cdot N_a / N_s$ to $V_o \cdot N_a / N_s$ in t_{D}. Since the output voltage value V_o is required, the best sampling point should be chosen as the end of t_{D}, which only contains information of the output voltage and winding ratio.

After that, the sampled output voltage is compared with an internal reference value via the voltage error amplifier EA_V, generating an error signal V_{COMV} that modulates the MOSFET duty cycle.

For constant-current regulation, the output current information is acquired by calculating the average of the diode current over a time period, which is expressed into $I_o = I_{\text{pk}} \cdot \frac{N_P}{N_S} \cdot \frac{t_{\text{D}}}{2t_s}$. By sampling the peak value of MOSFET drain-to-source current I_{pk} by a peak detector, the output current value can be derived through the estimator. Then the output current is compared with an internal reference value via the current error amplifier EA_I, generating an error signal V_{COMI} that modulates the MOSFET duty cycle. The output current information is then compared to a reference value and then an error signal V_{COMI} can be generated.

The smaller one of the two error voltages, V_{COMV} and V_{COMI} modulates the duty cycle D. Therefore, in constant voltage regulation mode, V_{COMV} decides the duty cycle while V_{COMI} is clamped to a high level; and in constant current regulation mode, V_{COMI} determines the duty cycle while V_{COMV} is clamped to a high level.

As a result, the voltage across auxiliary winding infers the output voltage and the current through MOSFET infers the output current. Primary side regulation regulates output voltage and current by detecting primary side information. This strategy eliminates the feedback loop from the secondary side, reduces numbers of components and decreases circuit losses.

5.2. FEEDBACK AND FEEDFORWARD CONTROL

THE quality of power supplies in global test laboratories are quite inconsistent. Some power supplies are highly accurate so they can provide stable input voltages; others may be out-of-date equipment that supply fluctuated input voltages. For pulse-width-modulation (PWM) DC-DC converters operated in continuous-current mode (CCM) and with no control, the output voltage is exactly proportional to the power supply input voltage, nearly irrelevant of the output current or load resistor.

Therefore, in those kinds of converters the measurement outcomes should be regulated to a constant level no matter how the input voltage changes, which is called line regulation.

Feedback control regulates the outputs with a negative feedback loop, while feedforward control uses the input voltage to predict its influence on the outputs. Comparing those two control methods and choosing a proper one is an important step in LED driver design.

5.2.1. FEEDBACK CONTROL

Conventionally, a negative feedback control scheme is applied on the circuit to adjust the output voltage against line voltage variations, as shown in Figure 5.3. The advantage of feedback systems over open-loop systems is that it not only makes the outputs insensitive to external disturbances like input voltage variations and load fluctuations, but also irrelevant to internal disturbances in system variables such as temperature. Therefore, the feedback loop can be designed to achieve very precise control, which is popularly used in electronic control systems such as amplifier circuits and oscillators.

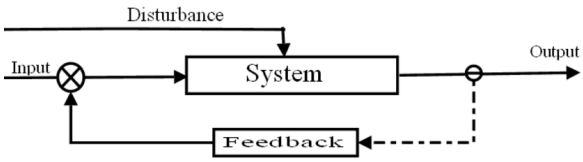

Figure 5.3: Feedback Diagram [3]. A controller compares the actual output of with the expected output value, and then converts the error into a control signal. In this way, the error can be minimized so that the output is adjusted back to the required response.

However, the most shortcoming of feedback control is that: the structure of the closed-loop system can be very complicated with more than one feedback loop in order to achieve highly accurate control results. Moreover, the system will probably become unstable or uncontrolled, if the gain of the controller is very sensitive to the fluctuation of input signals. The system will even begin to oscillate or fail to function and finally break out, as the controller tries to over-correct itself.

The feedback control has another disadvantage that makes it less ideal: it only takes action when there exists a deviation from the desired value. Thus, errors have already existed in the system before a feedback control is able to respond. In other words, the feedback controller starts too late so that it is incapable of adjusting a deviation at the exact time of its detection.

5.2.2. FEEDFORWARD CONTROL

The feedforward controller, also known as a predictive controller, is an effective and reliable technique capable of reacting before an error actually occurs. It measures the disturbances, uses it to foresee the influence on output, and reacts to its control signal in a pre-defined way without considering how the load behaves, see Figure 5.4. If how each change in disturbance affects the output can be described mathematically, then a math

model can be developed to design a preemptive control scheme that counteracts the predicted impact as the disturbances occur. Some prerequisites are needed for a reliable feedforward control scheme: the external command or controlling signal should be known, and the effect of system output on the load should be available.

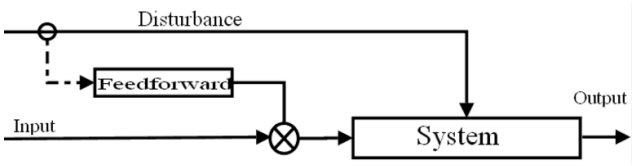

Figure 5.4: Feedforward Diagram [3]. The feedforward control measures the disturbances involved in the process and uses a mathematical model to eliminate the measurable disturbances.

In this method, the control variable adjustment is no longer error-based. Instead, it is based on information about the process in the form of a mathematical model and the measurements of the process disturbances. Therefore, the feedforward control can keep the output at reference value and eliminate the effects of measurable disturbances.

The greatest advantage of feedforward control is its fast dynamic response. For example, the correction for an input voltage perturbation takes action instantly, almost at the same time when the fluctuation happens. Furthermore, since the feedforward dynamics becomes independent from the compensation of the feedback loop, the possibility of fast-scale instability is much decreased. Also, feedforward control can help maintain the switching frequency or the loop gain of free-running converters at a stable level.

Therefore, feedforward control technique is most commonly used to improve line regulation in applications with wide ranges of input voltage. A typical example of the feedforward control method applied in DC–DC PWM boost converter operated in CCM has been proposed in [4].

As shown in Figure 5.5, for the PWM modulator, the peak value V_{Tm} of the sawtooth signal is kept constant at the non-inverting input and the reference voltage V_{REF} is set at the inverting input. The reference voltage V_{REF} follows the fluctuation of the input voltage V_{I} through a voltage divider R_1 and R_2:

$$V_{\mathrm{REF}} = \frac{R_1}{R_1 + R_2} \cdot V_{\mathrm{I}} \tag{5.1}$$

When V_{REF} is higher than the sawtooth signal V_{t}, the power transistor turns off; and when V_{REF} becomes lower than V_{t}, the power transistor turns on. Referring to Figure 5.5, the relationship between V_{REF}, V_{Tm} and D can be expressed as:

$$\frac{V_{\mathrm{Tm}}}{T} = \frac{V_{\mathrm{REF}}}{(1-D)\,T} \tag{5.2}$$

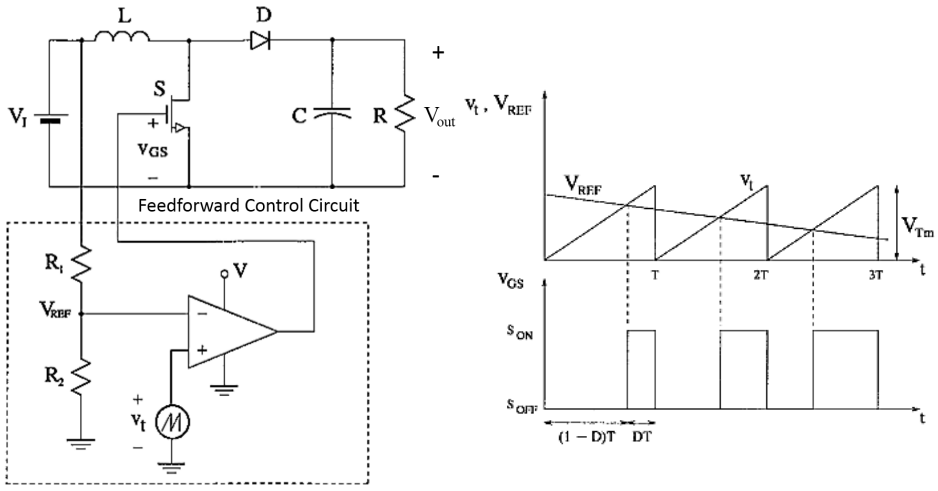

Figure 5.5: Feedforward control circuit and key waveforms for the boost PWM converter [4]. V_t is a ramp waveform and V_{REF} reflects the input voltage information. The switch is on when V_{REF} is lower than V_t. The feedforward control circuit regulates the output voltage independent of the input voltage.

Further, based on the operation principle of boost converter, the function between the input voltage V_I and the output voltage V_{out} is:

$$V_{out} = \frac{1}{1-D} \cdot V_I \tag{5.3}$$

With the combination of Equation 5.1, 5.2 and 5.3, the final expression of V_{out} can be written into Equation 5.4, which proves that V_{out} is independent of the input voltage V_I.

$$V_{out} = (\frac{R_1}{R_2} + 1) \cdot V_{Tm} \tag{5.4}$$

Consequently, the output voltage V_{out} only depends on the circuit parameters and the sawtooth voltage, independent of the input voltage V_I. The proposed feedforward control strategy can achieve precisely regulated output voltage and improve line regulation with no time delay as long as Equation 5.2 and Equation 5.3 are valid.

5.3. TRANSFER STANDARD CONTROL DESIGN

TRANSFER standard driver has been designed to be constant-power. Using secondary side regulation involves two feedback loops that detect and control two variables (voltage and current), which causes complexity to the circuit and adds uncertainties to the results. The opto-coupler needed for transferring electrical signals also adds extra components and power loss in the driver circuit. What's more, the error-based feedback control scheme can not take action at the exact time when the error happens. Controlling two variables also adds time delay to the control.

As a result, primary side regulation using feedforward is an optimal control strategy for the transfer standard LED lamp, in consideration of reliable control and simple topology.

REFERENCES

[1] S. Chen, E. Lan, and L. Lin, *Implementation of the primary-side regulation in flyback converters,* .

[2] Fairchild-Semiconductor, *Application note an-8033,* Design Guideline for Primary Side Regulated (PSR) Flyback Converter Using FAN103 and FSEZ13X7.

[3] Wikipedia, *Feed forward (control) — wikipedia, the free encyclopedia,* (2017), [Online; accessed 20-February-2017].

[4] M. K. Kazimierczuk and A. Massarini, *Feedforward control of dc-dc pwm boost converter,* IEEE Transactions on Circuits and Systems I: Fundamental Theory and Applications **44**, 143 (1997).

6

CONSTANT POWER CONTROLLER LM3447

IN this chapter, a constant power controller LM3447 is chosen based on the control requirements for the transfer standard LED lamp. The operational principles of LM3447 are validated by experiments. It is proved that LM3447 can achieve constant power measurement against temperature deviation.

6.1. TRANSFER STANDARD CONTROLLER SELECTION

BASED on the transfer standard criteria design in Chapter 4, the LED driver should be a constant-power driver because the transfer standard needs to rapidly reach a stable level of power and keep minimal fluctuation; according to the transfer standard control design in Chapter 5, the control scheme should be primary side control using feedforward in order to achieve reliable and instantaneous control with a simple topology and few components.

Texas Instruments (TI) provides a large portfolio of off-line LED lighting controllers. In May 2012, TI introduced a new LED controller with constant power regulation. The LM3447 AC/DC LED driver includes a dimmer detect, phase decoder and adjustable hold current circuits to provide smooth and flicker-free dimming operation in off-line, isolated LED lighting applications[1].

Conventional LED drivers normally apply constant current control to precisely regulate LED forward current, and thus generating the same light intensity which is comfortable to human eyes. However, under constant current when temperature increases during LED operation, forward voltage drops down and the electrical power decreases, so the LED efficacy decreases.

In comparison, by using LM3447 under constant power control, forward current goes up to offset the forward voltage drop due to temperature rise, keeping the electrical power at a constant value.

6.2. POWER FACTOR CORRECTION

6.2.1. FUNDAMENTALS

First consider a rectifier bridge with a storage capacitor, as shown in Figure 6.1a. The rectified voltage (in blue) is about 320 V and the load power dissipation is about 102 W. If the input current waveforms are sinusoidal, the current RMS value should be 0.445 A and peak value should be 0.629 A. However, the current results (in red) derived from simulation in Figure 6.1b show that the RMS value is 1.013 A RMS value and the peak value is about 4 A peak value. The power factor (PF) is 0.435 as calculated in LTspice.

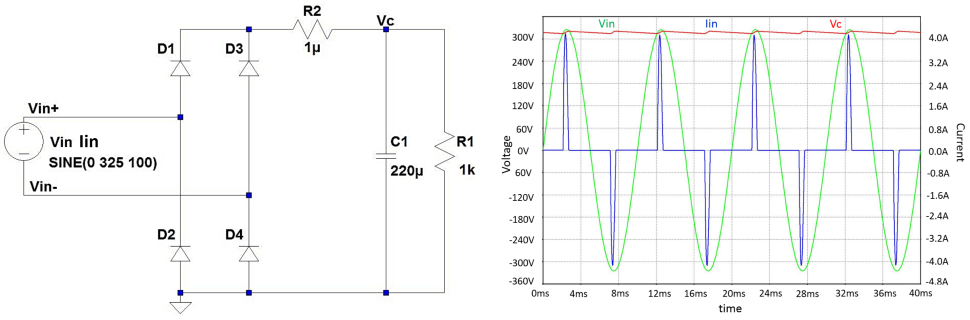

(a) (b)

Figure 6.1: An example of low power factor circuit. (a) A voltage source generates a sinusoidal voltage waveform whose peak value is 325 V and the frequency is 100 Hz. A rectifier bridge connected with a storage capacitor converts AC power to DC power and delivers the DC voltage to the load. (b) The sinusoidal waveform (in green) is the input voltage and the pulses (in blue) with 4 A peak values are input current waveforms. The flat DC voltage (in red) is the output voltage.

From simulation results, input current waveforms are made up of several narrow pulses with large peak values. That also means a large amount of current needs to be extracted from the mains to deliver the needed power to the load. Large current leads to higher energy loss and lower system efficiency.

Switched-mode-power-supplies (SMPS) present nonlinear impedance, so power factor correction circuit is needed. In SMPS, the input side usually involves a rectifier circuit following a storage capacitor. This capacitor keeps voltage approximately around the peak value of input wave until the next peak arrives to refill the capacitor. Therefore, current only flows near the peaks of the input waveform, in the form of several pulses. Every current pulse contains large energy to sustain the load until the next peak, by charging the capacitor for a pulsed time and then discharging the stored energy to the load for the rest time in the cycle. Commonly, the current pulse can be 10 % to 20 % of the cycle, which means the pulse carries 5 to 10 times the average current.

Power factor (PF) is defined as the ratio of real power to apparent power, in which the real power P is the average of the instantaneous product of voltage and current, and the apparent power S is the product of the rms value of voltage and current. When both voltage and current are pure sine waves and in phase with each other, the power factor is unity.

Power factor Correction (PFC) shapes the input current of the power supply to a nearly sinusoidal waveform, in order to maximize the real power extracted from the power source. Ideally, the electrical device should display a load characteristic of a pure resistor, where the reactive power is zero. In this case, the input current is reshaped to a similar waveform as the input voltage (mostly a sine wave) and is also exactly in phase with it. As a result, the current generated by the power supply is at a minimum value for the real power required from the load, at the same time reducing the power loss and minimizing the system cost.

Active power factor correction makes the input current to match the shape of the input voltage waveform, by inserting a switched-mode boost or flyback converter controlled by a PFC IC (Integrated Circuit) between the rectifier and the storage capacitor.

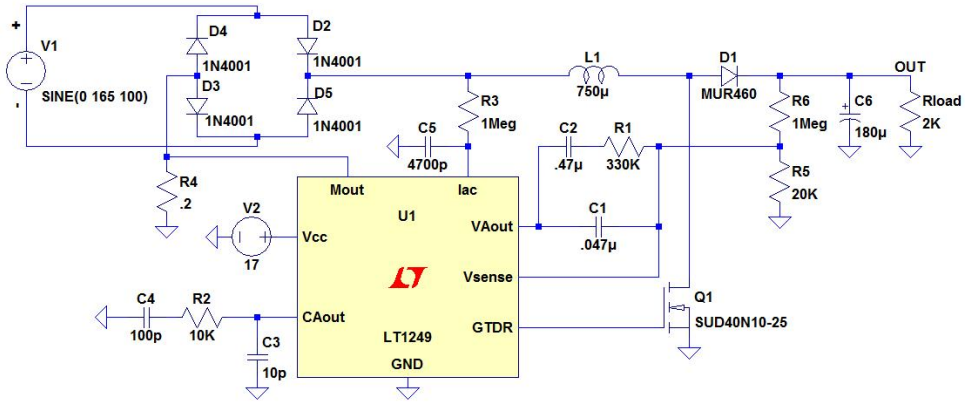

Figure 6.2: High power factor circuit built in LTspice. By inserting the power factor controller LT1249 between the rectifier and the boost converter, power factor can be regulated high.

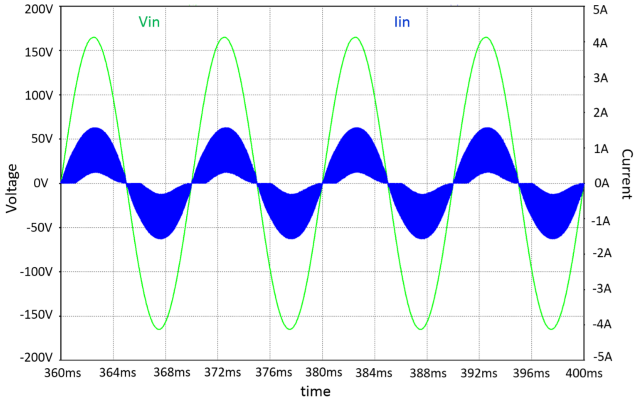

Figure 6.3: The input voltage and current waveforms of the high power factor circuit. The sinusoidal waveform (in green) is the input voltage. The input current waveform (in blue) follows the shape of the input voltage because of the power factor controller LT1249.

A circuit based on power factor controller LT1249 is built in LTspice to study active power factor correction, as shown in Figure 6.2. Figure 6.3 illustrates the input voltage (in green) and input current (in blue) waveforms under PFC. In practice, the filtering of the input current would be conducted by an EMI filter to produce a smooth average current waveform. Therefore, the input current becomes a nearly perfect sine wave and in phase with the input voltage. The power factor is 0.915 calculated in LTspice.

6.2.2. POWER FACTOR CORRECTION IN LM3447

In LM3447, the power factor correction is realized by inserting a flyback converter which operates in discontinuous conduction mode (DCM). A typical primary side power regulated Flyback LED driver using LM3447 is shown in Figure 6.4.

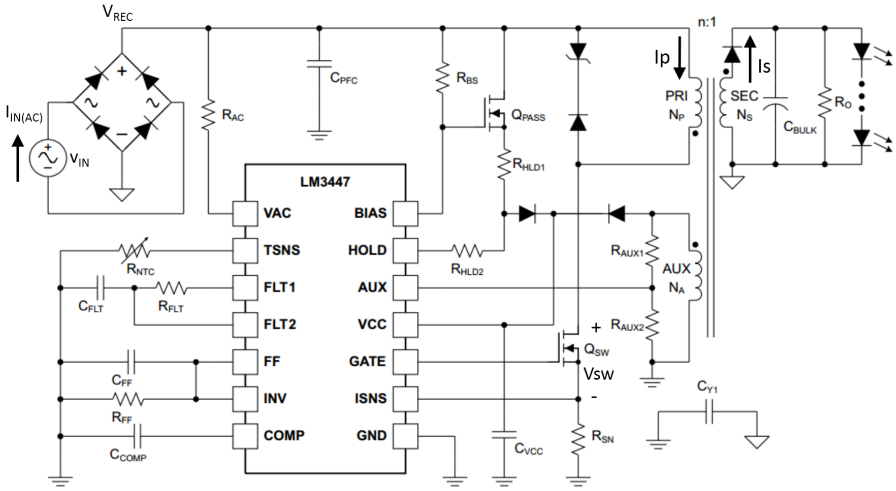

Figure 6.4: A typical primary side power regulated Flyback LED driver circuit. The driver is supplied by an AC voltage source V_{IN}. LM3447 is inserted into the circuit between the rectifier and the Flyback converter to achieve power factor correction and primary side regulation.

When the switch is on, the primary current I_P rises linearly from zero to $I_{P(PK)}$; when the switch is off, the secondary side current I_S decreases from $I_{S(PK)}$ to zero, see the waveforms in Figure 6.5b. In this operation mode, the peak value of the primary current $I_{P(PK)}$ is given by:

$$I_{P(PK)} = \frac{v_{REC}(t)}{L_M} \cdot DT_s = \frac{|v_{in}(t)|}{L_M} \cdot DT_s \tag{6.1}$$

where, $v_{in}(t) = V_{IN(PK)} \sin\left(\frac{2\pi}{T_L} t\right)$ is the AC input voltage, $v_{REC}(t)$ is the rectified input voltage, L_M is the transformer magnetizing inductance referred to the primary side winding, D is the duty cycle, T_s is the switching period and T_L is the line period.

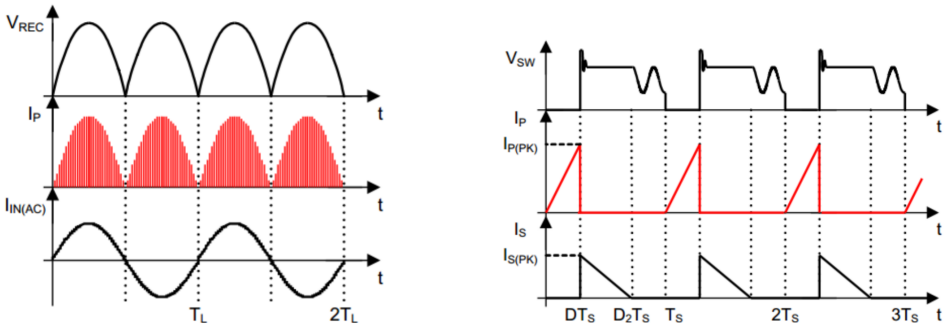

(a) (b)

Figure 6.5: Key waveforms of Flyback operating in discontinuous conduction mode [2]. (a) Over line period, voltage waveforms after rectification V_{REC} are half sine waves and the contour of the primary current I_P follows the shape of V_{REC}. The input current waveform is sinusoidal and in the same phase with the input voltage, which proves the power factor correction. (b) Over switching period, I_P rises up when the switch is on. I_S drops down when the diode at the secondary side is on. I_P and I_S keep zero when the switch and the diode are both off.

For a constant switching frequency controller, if the duty cycle D is held constant over a line cycle, then the peak primary current, $I_{P(PK)}$, is proportion to the magnitude of the voltage at the output of the bridge rectifier $v_{REC}(t)$. Therefore, the contour of the primary current I_P exactly follows the shape of rectified input voltage v_{REC}, which is a rectified sine wave, as shown in Figure 6.5a.

The average primary current $I_{P(AVG)}$ is obtained by averaging the area under I_P over the switching period T_S:

$$I_{P(AVG)} = \frac{1}{T_S}\int_0^{T_S} I_P\,dt = \frac{1}{2}\cdot\frac{|v_{in}(t)|}{L_M}\cdot D^2 T_s \tag{6.2}$$

Because in a practical implementation of the active rectifier, the filtering of the input current would be performed by an EMI filter to produce the smooth average current waveform, so the resulting input current $i_{in}(t)$ is considered equal to the average current $I_{P(AVG)}$ in the positive half cycle and $-I_{P(AVG)}$ in the negative half cycle:

$$i_{in}(t) = \frac{1}{2}\cdot\frac{v_{in}(t)}{L_M}\cdot D^2 T_s \tag{6.3}$$

The input current $i_{in}(t)$ exactly emulates the input voltage $v_{in}(t)$, in a sinusoidal waveform and in the same same phase. As a result, the DCM flyback converter behaves much like a pure resistor and exhibits a power factor close to unity, achieving power factor correction.

The input power P_{IN} drawn by the flyback PFC can be derived by averaging the product of input voltage $v_{in}(t)$ and input current $i_{in}(t)$, over half line cycle $T_L/2$:

$$
\begin{aligned}
P_{\mathrm{IN}} &= \frac{2}{T_L}\int_0^{\frac{T_L}{2}} v_{\mathrm{in}}(t)\cdot i_{\mathrm{in}}(t)dt \\
&= \frac{2}{T_L}\int_0^{\frac{T_L}{2}} \frac{1}{2}\cdot\frac{V_{\mathrm{IN(PK)}}^2 D^2 T_s}{L_{\mathrm{M}}}\cdot sin^2(\frac{2\pi}{T_L}t)dt \\
&= \frac{1}{4}\cdot\frac{V_{\mathrm{IN(PK)}}^2 D^2 T_s}{L_{\mathrm{M}}} \\
&\propto (V_{\mathrm{IN(PK)}}\cdot D)^2
\end{aligned}
\tag{6.4}
$$

In the expression of the input power P_{IN} in Equation 6.4, for DCM flyback converter, the input power is relevant to elements: the peak input voltage $V_{\mathrm{IN(PK)}}$, the duty cycle D, the switching period T_s and the transformer inductance L_{M}. In this case,the flyback converter operates in fixed switching frequency, so the input power P_{IN} is in proportional to the product of the peak input voltage and the duty cycle $V_{\mathrm{IN(PK)}}\cdot D$. Keeping the input power at a stable level means maintaining the product of $V_{\mathrm{IN(PK)}}\cdot D$ constant by control scheme in the whole operation process.

6.2.3. TEST ON POWER FACTOR CORRECTION

To verify the power factor correction (PFC) performed by the LM3447, the waveforms of input voltage and input current are captured and recorded. The input voltage generated by a power supply is a sine wave, while the input current is not sinusoidal because of the nonlinear impedance. Observe whether the input current is in the same shape and phase with the input voltage. Record the value of total harmonic distortion factor (THD) and the power factor (PF) to check the quality of the waveforms. LM3447-PAR-230VEVM recommended test setup is shown in Figure 6.6.

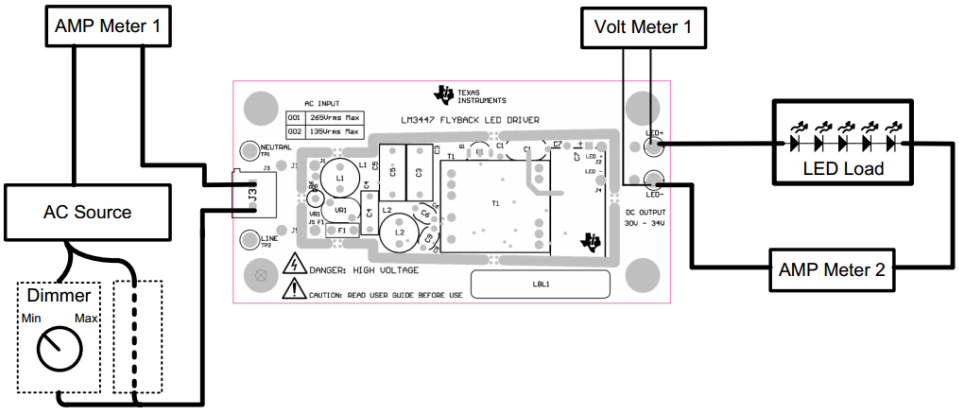

Figure 6.6: Test setup [3]. The input port of the evaluation board is connected to the power source. The output port of the board is connected to the load. Test point LED+ is connected to LED anode and test point LED- is connected to LED cathode.

The test equipment involves:

1. AC source: Pacific Power AMX108 AC power source
2. Multimeters: FLUKE 179 True RMS Multimeter
3. Oscilloscope: Tektronix TDS 2024C four channel digital storage oscilloscope
4. Load: four 330 Ω resistors in parallel and connected in series with a variable resistor
5. Operating temperature: 23 °C

In this experiment, four 330 Ω paralleled resistors and a variable resistor are used to replace LED load and to simulate change in LED load resistance with temperature deviation.

In the first step, set the input voltage $V_{\text{in(rms)}}$ to 185V and load resistance at 82.5 Ω. Measure the input voltage and input current. In Figure 6.7a, the input voltage waveform (in red) and the input current (in blue) are approximately in the same shape and phase with each other, so LM3447 performs well in power factor correction.

What's more, it can observed from the waveforms that the input current waveform has a little distortion near its peaks. This distortion in the input current waveform means that harmonics exist in the current which leads to the non-unity power factor value. The reason is that the filtering of EMI is not able to completely eliminate all of the harmonic currents, so that certain high harmonic currents are left behind.

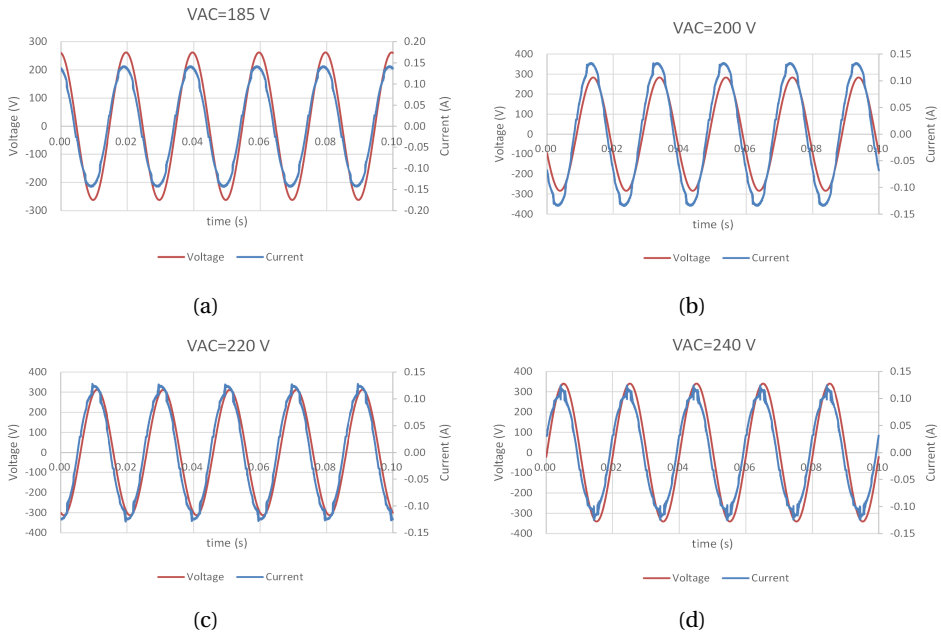

Figure 6.7: Input voltage and input current waveforms when RMS values of input voltages are different. Input voltages are perfectly sinusoidal and input currents are in the same phase with input voltages, but current waveforms distort as the input voltage increases. (a) $V_{\text{in(rms)}}$=185 V. (b) $V_{\text{in(rms)}}$=200 V. (c) $V_{\text{in(rms)}}$=220 V. (d) $V_{\text{in(rms)}}$=240 V

In the next step, in order to investigate the power factor correction behavior under various input voltages, different $V_{in(rms)}$ are set and the waveforms are compared, see Figure 6.7. The input voltages are always sine waves because they are generated by the power supply. Under all values of $V_{in(rms)}$, input currents and voltages are almost in uniform phase. However, the distortion of input current becomes more and more serious as the input voltage increases. Especially when $V_{in(rms)}$ is 240 V, the shape of input current is even sharp around its peaks, far away from sinusoidal. It shows that the power factor correction degrades with the increasing input voltage.

Table 6.1: THD and PF under various input voltages

$V_{in(rms)}$/V	185	200	220	240
THD %	3.153	3.492	4.187	4.903
PF	0.984	0.978	0.969	0.960

To better illustrate the trend of power factor correction with the change of input voltage, record the values of THD and PF under four circumstances of input voltages in Table 6.1. The increase of THD and decreases of PF also prove that current harmonics become severe with the the change of the input voltage.

6.3. CONSTANT POWER CONTROL SCHEME

6.3.1. FUNDAMENTALS

LM3447 regulates constant power by primary side control using input voltage feedforward strategy. This control scheme can achieve reliable regulation of input power against the change of LED load resistance over temperature deviation and lifetime. The constant power control in LM3447 increases luminous efficacy with simple topologies and fewer components.

A mathematical model describing the disturbances to the system can be used to predict the error in feedforward control scheme. More details of primary side regulation and feedforward control have already been illustrated in Chaper 5, so the fundamentals will not be explained here any more.

6.3.2. CONSTANT POWER CONTROL IN LM3447

The LM3447 integrates an innovative primary side input power regulation scheme based on input voltage feedforward control techniques. The control scheme uses the duty cycle D as the control variable for regulation. The duty cycle is generated using an internal error amplifier and a fixed frequency, triggered ramp generator. The feedforward loop consisting of input voltage sensing circuit, the input feedforward block, the error amplifier and PWM comparator, is able to resist any input voltage perturbation by adjusting the duty cycle, thus realizing tight line regulation. The rectified input line voltage is fed to the controller to realize input voltage feedforward as shown in Figure 6.8.

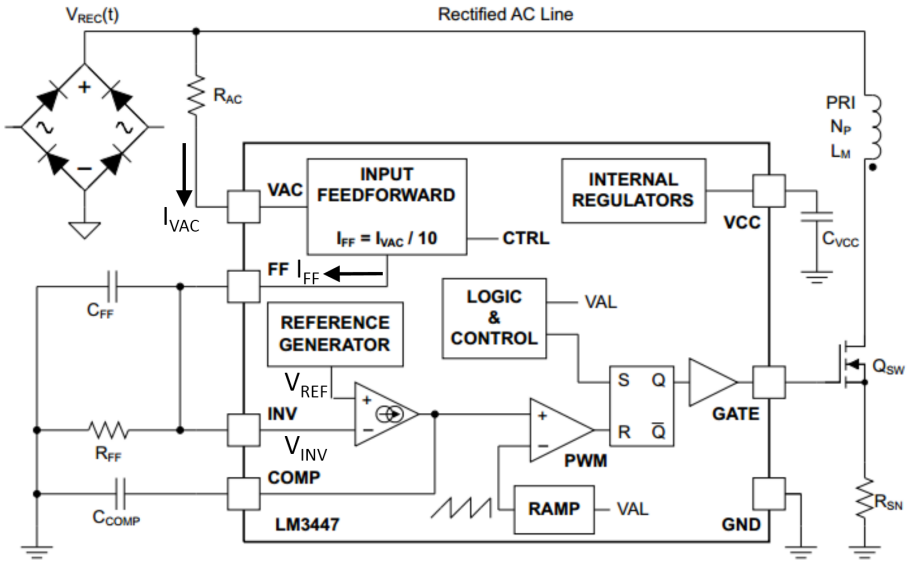

Figure 6.8: Feedforward control circuit [2]. The rectified input voltage V_{REC} is detected by a sense resistor R_{AC} at the rectified AC line, converted to a current signal I_{VAC} and sent into the Input Feedforward diagram. Afterwards, a current signal I_{FF} drawn from the Input Feedforward diagram is filtered by a parallel resistor R_{FF} and capacitor C_{FF} at the FF pin, as the input information V_{INV} of the internal error amplifier. An error is generated because of the difference between V_{INV} and the reference voltage V_{REF}. The PWM comparator compares this error to a ramp waveform, generating the gate signal to the switch.

6.3.3. TEST ON CONSTANT POWER CONTROL

In order to verify the input feedforward regulation of LM3447, measure the control variable D under different input voltages to see how it is adjusted to realize constant input power.

TEST WHEN $V_{IN(RMS)}$=230 V

Set the input voltage $V_{in(rms)}$ to 230 V. Measure the waveforms of input voltage V_{in} and the primary current I_P, see Figure 6.9. The input voltage V_{in} (in blue) is a sine wave generated by the input source. Its peak value $V_{IN(PK)}$ is about 325 V in measurement, considering the amplification factor 20 of the differential probe. The period of the input voltage is 20 ms, and the line frequency is 50 Hz. The primary current I_P (in yellow) is a series of triangular waveforms whose contour follows the rectified input voltage, which can prove the power factor correction of the circuit.

Zoom in and select three positions of the input voltage: maximum, middle and minimum, as shown in Figure 6.10. The primary current I_P linearly increases as the switch is on and keeps zero as the switch is off. The switching frequency is measured to be 69 kHz. The overshoot in the waveforms of I_P is due to the transition of switching behavior.

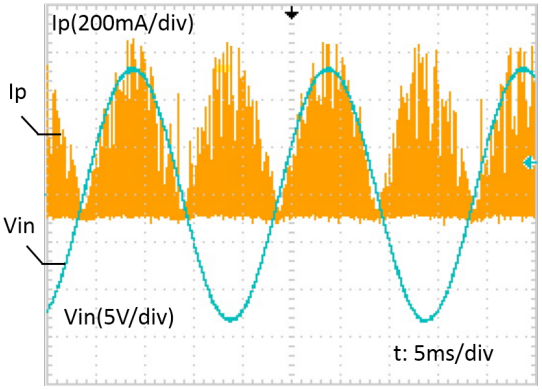

Figure 6.9: When RMS value of the input voltage is 230 V, input voltage waveform (in blue) is sinusoidal and primary current waveforms (in yellow) are half sine waves that follow the shape of the rectified input voltages.

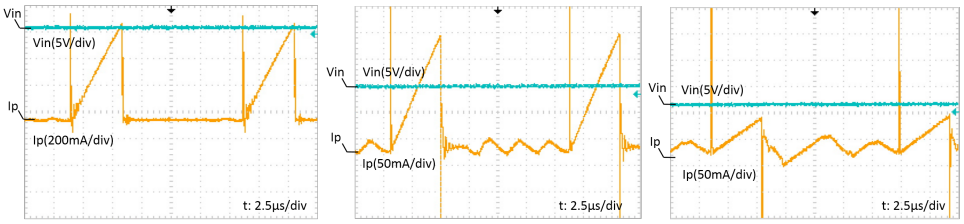

(a) (b) (c)

Figure 6.10: When RMS value of the input voltage is 230 V, zoom in the input voltage waveforms (in blue) and primary current waveforms (in yellow). The primary current rises up when the switch is on. The duty cycle can be figured out by measuring the rising time of the primary current. (a) The input voltage is at its maximum value. (b) The input voltage is at its middle value. (c) The input voltage is at its minimum value.

Measure the duty cycle D, which is the time interval when I_P linearly rises. Record the peak value of the primary current $I_{P(PK)}$ at three positions of the input voltage. The results are listed in Table 6.2.

Table 6.2: Duty cycle and peak primary current at three positions of the input voltage

	$v_{in}(t)$/V	D	$I_{P(PK)}$/mA
MAX	350	0.28	720
MID	100	0.28	220
MIN	30	0.28	70

When $V_{in(rms)}$ is set at a constant value 230 V, the conclusions about duty cycle and peak value of primary current derived from Table 6.2 are given below:

1. The duty cycle D is all the time 0.28, which proves the constant duty cycle operation of the LM3447 when the input voltage is at a specific value.

2. The peak value of primary current $I_{P(PK)}$ is proportional to the instantaneous value of input voltage $|V_{in}|$ when D is constant, as expected in Equation 6.1: $I_{P(PK)} = \frac{|v_{in}(t)|}{L_M} \cdot DT_s \propto |v_{in}(t)|$.

TEST WHEN $V_{IN(RMS)}$=185 V

Change the input voltage $V_{in(rms)}$ to be 185 V and do measurements in the same procedure as when $V_{in(rms)}$ is 230 V. The waveforms of input voltage V_{in} and the primary current I_P are given in Figure 6.11. The input voltage V_{in} (in blue) is a sine wave whose peak value $V_{IN(PK)}$ is 260 V in measurement. The contour of primary current I_P (in yellow) follows the shape of rectified input voltage, which can prove the power factor correction of the circuit.

The zoomed in waveforms when input voltage is at three positions are shown in Figure 6.12. The results of duty cycles and the peak values of the primary current are listed in Table 6.3.

Conclusions about constant duty cycle operation and proportional peak value of primary current to the input voltage can in the same way be derived from Table 6.3.

Table 6.3: Duty cycle and peak primary current at three positions of the input voltage

	$v_{in}(t)$/V	D	$I_{P(PK)}$/mA
MAX	260	0.34	720
MID	160	0.34	460
MIN	40	0.34	110

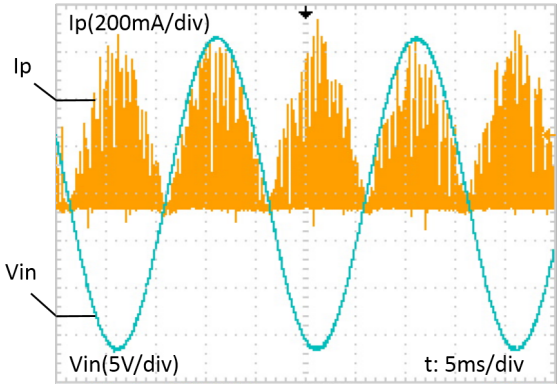

Figure 6.11: When RMS value of the input voltage is 185 V, input voltage waveform (in blue) is sinusoidal and primary current waveforms (in yellow) are half sine waves that follow the shape of the rectified input voltages.

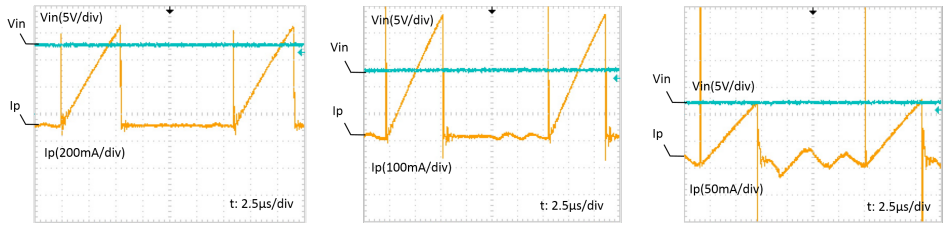

(a) (b) (c)

Figure 6.12: When RMS value of the input voltage is 185 V, zoom in the input voltage waveforms (in blue) and primary current waveforms (in yellow). The primary current rises up when the switch is on. The duty cycle can be figured out by measuring the rising time of the primary current. (a) The input voltage is at its maximum value. (b) The input voltage is at its middle value. (c) The input voltage is at its minimum value.

COMPARE TESTS WHEN $V_{IN(RMS)}$=230 V AND $V_{IN(RMS)}$=185 V

To investigate how the duty cycle is adjusted by the input feedforward control scheme as the input voltage fluctuates, compare the duty cycles under two different input voltages. The results in Table 6.4 shows that when the input voltage $V_{IN(PK)}$ varies from 325 V to 260 V, the duty cycle D changes from 0.28 to 0.34 so that the product $V_{IN(PK)} \cdot D$ is maintained at a constant value around 90 and the input power is also be maintained at about 16 W. That proves the feasibility of input power regulation. The error may come from the oscilloscope.

Table 6.4: Comparison under two input voltages

$V_{IN(PK)}$/V	D	$V_{IN(PK)} \cdot D$	P_{IN}/W	$I_{P(PK)}$/mA
325	0.28	90.0	16.20	720
260	0.34	89.4	16.09	720

In the further step, the peak value of primary current $I_{P(PK)}$ is investigated under two input voltages. It changes with the instantaneous value of the input voltage and its contour follows the shape of rectified input voltage when the circuit conducts in constant duty cycle operation mode. However, under varying input voltage and duty cycle, $I_{P(PK)}$ is relevant to the product $V_{IN(PK)} \cdot D$, based on the expression $I_{P(PK)} = \frac{|v_{in}(t)|}{L_M} \cdot DT_s \propto |v_{in}(t)| \cdot D$. Because $V_{IN(PK)} \cdot D$ is ensured constant due to input feedforward control, $I_{P(PK)}$ is also stable at the same position of input voltage. For example, the values of $I_{P(PK)}$ are both 720 mA when two input voltages reaches maximum levels , as shown in Table 6.4.

6.4. LINE REGULATION AND LOAD REGULATION

6.4.1. LINE REGULATION

Line regulation is defined as the ability of the power supply to keep a constant output voltage level in spite of the input voltage variation. This ability is very important when

the power source is unstable or unregulated, because changes in line voltages can generate a disproportional variation in output voltage and output current. For LEDs, its light output is proportional to current and is rated for a current range. If current exceeds the manufacturer recommendations, the LEDs can become brighter, but their light output can degrade at a faster rate due to higher temperatures within the device which leads to a shorter lifespan. So LED light bulbs must be resistant of line voltage fluctuations during operation. A low line regulation is always preferred. In practice, a well regulated power supply should have a line regulation of at most 0.1 %.

In order to investigate the line regulation performed by LM3447, select different values of input voltages, and check whether the corresponding output voltages can be maintained at a stable level. Here, the load is a pure resistor of 82.5 Ω.

In the first step, set the input voltage at 185 V and measure the output voltage V_{out} waveform by an oscilloscope. As shown in Figure 6.13, V_{out} is not constant and has a voltage ripple on it, which is because the output capacitor is being charged and discharged over one half line cycle. The frequency of V_{out} is 100 Hz, twice as the line frequency 50 Hz. The average value of V_{out} is 36.33 V, and the corresponding output power P_{out}, input power P_{in} and efficiency η are calculated.

Table 6.5: Line regulation

$V_{in(rms)}$ / V	V_{out} / V	P_{out} / W	P_{in} / W	η
185	36.33	16.00	18.21	0.88
230	36.37	16.03	18.21	0.88
240	36.41	16.07	18.26	0.88

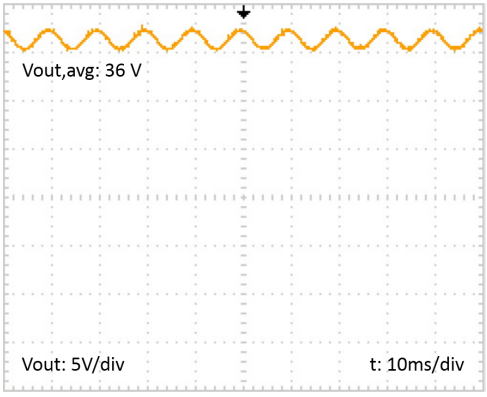

Figure 6.13: Output voltage waveform when V_{in} is 185 V. The average value of V_{out} is about 36 V. V_{out} has a voltage ripple on it. The frequency of V_{out} is 100 Hz, twice as the line frequency 50 Hz.

In the next step, change the values of input voltages and record the output voltage waveforms to see whether V_{out} is stable. From Table 6.5, it can be concluded that V_{out} does not differ much as the change of V_{in}, which proves the effectiveness of line regula-

tion of LM3447. Moreover, thanks to the input feedforward regulation, the input power is kept at a stable level around 18.2 W. And the conversion efficiency is always about 0.88.

6.4.2. LOAD REGULATION

Another important specification for an LED driver is load regulation, the capability of a power supply to maintain a constant voltage level in spite of the load fluctuation. During operation, LED load resistance changes with temperature rising. Therefore, a good LED driver should have the ability of withstanding the fluctuation in the load resistance and maintaining a stable output.

The first step in investigating load regulation in LM3447 is to define the range of load resistance across operating temperatures. To figure out how far the LED resistance changes with temperature variation, study the temperature effects on LED forward characteristics by applying Shockley's equation 6.5, where I_S is reverse saturation current, k is Boltzmann's constant, q is electron charge and T is temperature in Kelvin.

$$I_D = I_S\left(e^{\frac{qV}{kT}} - 1\right) \tag{6.5}$$

To investigate the temperature effects on LED characteristics in reality, IV curves are plotted under two different temperatures 30 °C and 70 °C. The method is to set constant current values and measure the resulting voltage values, see Figure 6.14. Those two points of temperature are selected in order to model the real situation of LED operation, that is 30 °C of around ambient temperature (in red) and 70 °C after long time operating (in blue). IV curve shifts to the left side (from the red to the blue) when temperature goes up.

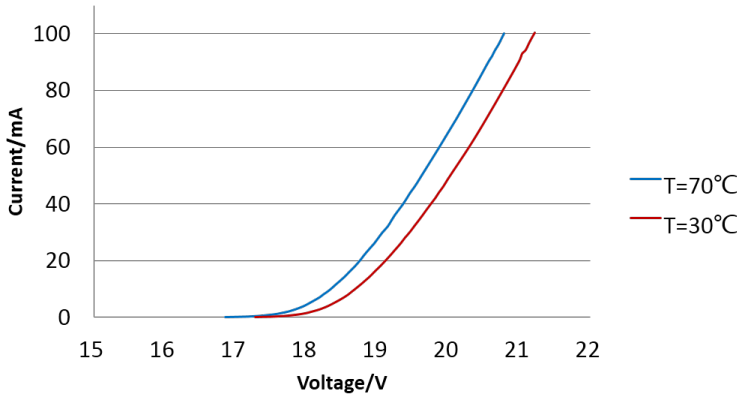

Figure 6.14: Measurement results of I-V curves under 30 °C and 70 °C. The I-V curve shifts to the left side when temperature rises from 30 °C to 70 °C.

Then calculate the LED equivalent resistance at each point. Current values are sourced and voltage values are measured at each test point. At the same current values, voltage

values decrease as the temperature rises, so the LED equivalent resistance increases. The percentages of resistance change are also calculated. It can be seen that the change of LED equivalent resistance normally do not exceed to 2 % when temperature rises from 30 °C to 70 °C. Therefore, the change of LED equivalent resistance in normal operation can be estimated as 2 %.

Since LED resistance varies within 2 %, load resistance in this test can be changed from 82.5 Ω to 84.5 Ω. Keep a constant input voltage, change the load resistance and then measure the output voltage to see whether it is constant as expected.

Table 6.6: Load regulation

R/Ω	V_{out}/V	P_{out}/W	P_{in}/W	η
82.5	36.37	16.04	18.21	0.88
83.5	36.58	16.03	18.21	0.88
84.5	36.79	16.02	18.21	0.88

The results in Table 6.6 show that output voltages can keep stable around 36 V when load resistance changes from 82.5 Ω to 84.5 Ω, which proves load regulation in LM3447. In the same word, LED resistance fluctuation with temperature has no influence on LM3447's output voltages and input power values.

6.5. OVERCURRENT AND OVER VOLTAGE PROTECTION

6.5.1. OVERCURRENT AND SHORT CIRCUIT PROTECTION

The LED driver circuit needs overcurrent protection (OVP) to prevent the entire system from shutting down in case of short circuit conditions. Current exceeding the recommended maximum value would cause the heat problem or break out. The LM3447 provided short circuit protection by sensing the current through the switching transistor Q_{SW} via a sense resistor R_{SN} series connected to the source of switch, as shown in Figure 6.15. The sense resistor R_{SN} converts the current flowing through the source of switch to a voltage signal, which is monitored at ISNS pin for overcurrent sensing.

At the beginning of every switching cycle, the Leading Edge Blanking (LEB) diagram pulls the ISNS input to a low level for about 170 ns in order to avoid false starting of the protection circuit due to voltage overshoot caused by switch turn on transitions. The cycle-by-cycle current limitation is achieved by comparing the sensed voltage at ISNS pin with the internal 275 mV overcurrent protection threshold. When the sense voltage reaches 275 mV, the switch is instantaneously switched off for 812 ms set by the fault timer. Under fault circumstances, the LM3447 operates in a hiccup mode, trying to restart the circuit after a time interval of 812 ms. As soon as the fault is cleared out, normal operation restarts.

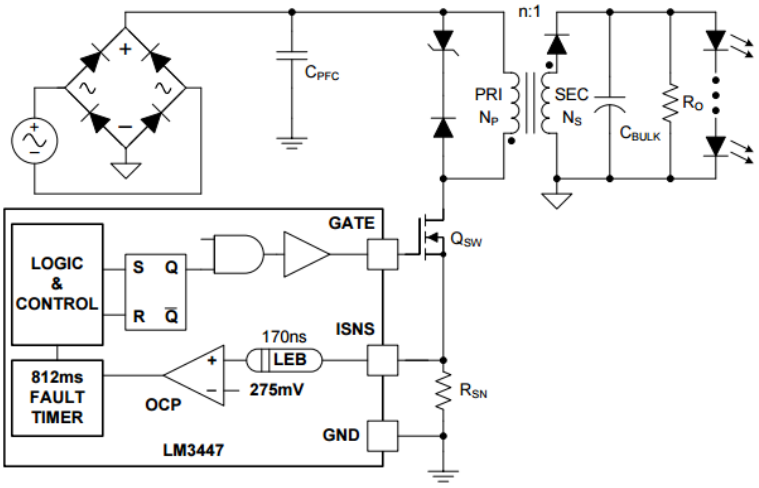

Figure 6.15: Current sense circuit [2]. A sense resistor R_{SN} is connected to the switching transistor Q_{SW} and converts the current flowing through the source of switch to a voltage signal sending to ISNS pin for overcurrent sensing.

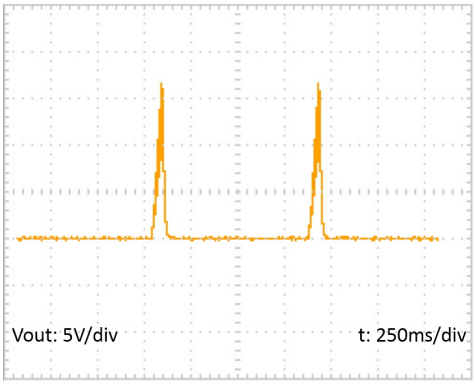

Figure 6.16: Output voltage waveform in short circuit experiment. The output voltage falls down when the current sense circuit detects overcurrent, and the period is measured as about 820 ms, which is consistent with the time period 812 ms illustrated in the datasheet. The experiment shows that when the load resistance is below 19.8 Ω, the circuit starts overcurrent protection.

The overcurrent limit I_{LIM} is written into Equation 6.6, in which V_{TH} is the overcurrent protection threshold fixed by the internal comparator and R_{SN} is the selected resistance. By choosing sense resistor R_{SN}, the overcurrent limit can be set at a required value. The threshold voltage V_{TH} is 275 mV, known from the block diagram of the current sense circuit shown in Figure 6.15. The sense resistor R_{SN} is 0.18 Ω, according to the schematic shown in [3]. Therefore, the overcurrent limit I_{LIM} is about 1.53 A. The short circuit experiment is conducted and the output voltage waveform is shown in Figure

6.16.

$$I_{LIM} = \frac{V_{TH}}{R_{SN}} \tag{6.6}$$

6.5.2. OVERVOLTAGE AND OPEN CIRCUIT PROTECTION

The LED circuit also needs protection against an overvoltage condition. The purpose of the overvoltage protection (OVP) circuit is to detect and then quickly pull down the overvoltage condition to prevent damage to the device. The LM3447 has a built-in overvoltage protection (OVP) mode to protect VCC from exceeding its maximum rating under open circuit conditions.

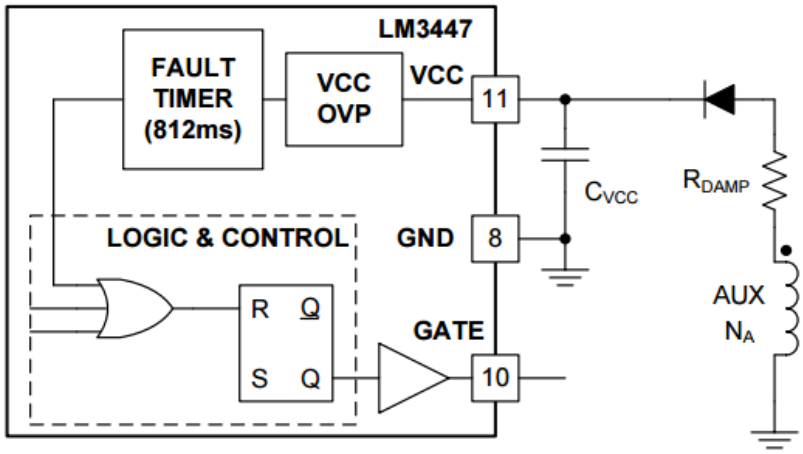

Figure 6.17: Overvoltage protection circuit [2]

In Figure 6.17 the voltage at the auxiliary winding reflects the information of output voltage, so that it is delivered to VCC pin for overvoltage sensing. The VCC voltage is monitored by a comparator with a rising threshold of 18.9 V and 175 mV of hysteresis. Upon detecting an over voltage situation, GATE pin is pulled to a low level for duration of 812 ms, determined by the internal fault timer. Once the fault is cleared up, the fault timer is then disabled and normal operation mode resumes. An optional damping resistor R_{DAMP} in series with the auxiliary winding can be used to prevent transformer leakage current from peak charging the capacitor C_{VCC} and false triggering the OVP circuit. Based on the magnitude of leakage inductance a resistor of 10 Ω to 47 Ω should provide proper damping.

The open circuit experiment shows that when the load resistance is over 86 Ω the circuit conducts overvoltage protection. The output voltage waveform in open circuit situation is shown in Figure 6.18.

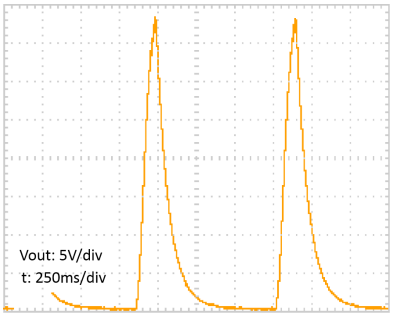

Figure 6.18: Output voltage waveform in open circuit experiment. Every time the output voltage rises to the threshold voltage 38 V, the open protection takes action and turns off the switch. After the time interval of 812 ms, the circuit restarts so the switch turns on and the output voltage increases again. Since the open circuit problem still exists, the protection operates every 812 ms so that the output voltage goes up and down in each cycle.

6.6. OVERALL TEST ON LM3447

THE objective of this test is to investigate the input power variation with the change of time and temperature on LM3447 evaluation board. In the first step, the load resistance is chosen at a fixed value, in order to simulate the situation when the temperature becomes stable so that the load is not influenced by the temperature deviation.

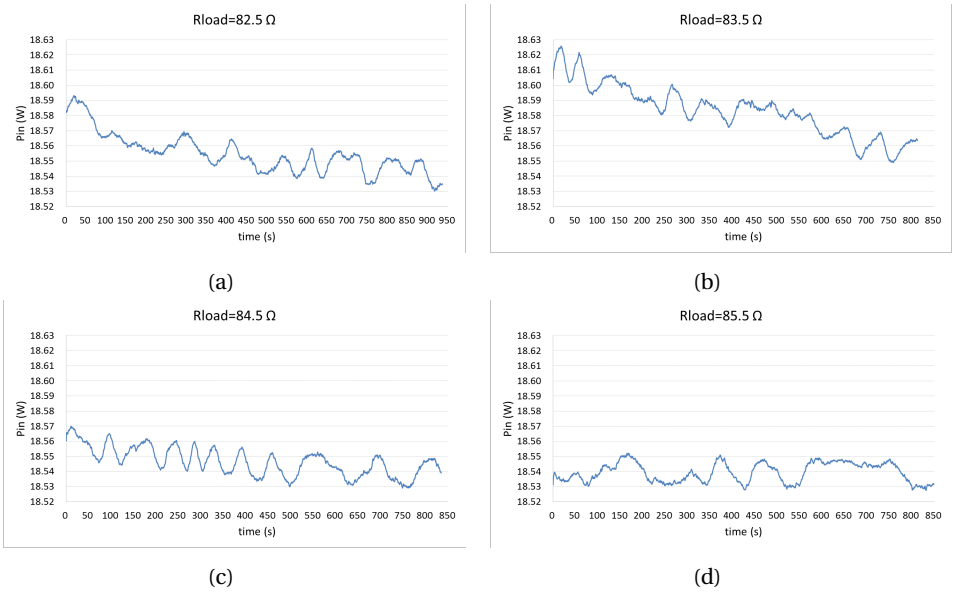

Figure 6.19: Input power variation with time under different load resistance. (a) Load resistance is 82.5 Ω. (b) Load resistance is 83.5 Ω. (c) Load resistance is 84.5 Ω. (d) Load resistance is 85.5 Ω.

When the load resistance is 82.5 Ω, measure the input power and observe how it changes with time. If the input power can keep stable under a specific load resistance, it means the power constant regulation works well when the temperature becomes stable. As shown in Figure 6.19a, the input power goes down at beginning, since the load resistance is influenced by temperature deviation. In the following time, the input power keeps oscillating around a stable level.

The load resistance is changed and the measurement results are recorded in Figure 6.19b-6.19d. When the load resistance is increased to 85.5 Ω, the input power does not decrease at beginning since the test has been conducted for a long time and the temperature has already been stable. From the maximum and minimum input power and the difference between them recorded in Table 6.8, it can be proved that the input power variation can be restricted within 0.4 % on LM3447 test board after thermal stability.

In the next step, the input power variation is compared under different load resistances. The LED resistance variation due to the temperature deviation is modeled by the change of load resistance. For example, the load resistance is changed from 82.5 Ω to 84.5 Ω, about 2.42 % variation. Under constant-voltage (CV) or constant-current (CC) control, the input power variation is estimated as 2.42 %, the same as the load resistance variation. In comparison, under constant-power control, the input power fluctuates between 18.59 W and 18.53 W, about 0.32 % variation.

Table 6.7: Input power under different load resistance

R/Ω	P_{max}/W	P_{min}/W	P_{avg}/W	$\Delta P/W$	$\Delta P/\%$
82.5	18.59	18.55	18.53	0.06	0.33
83.5	18.62	18.58	18.55	0.07	0.41
84.5	18.57	18.55	18.53	0.04	0.22
85.5	18.55	18.54	18.53	0.02	0.13

Table 6.8: Input power under different load resistance

$\Delta R/\%$	$\Delta P_{avg}/W$	$\Delta P_{avg}/\%$
2.42 %	0.008	0.04 %

Furthermore, the standard deviation of the input power has been calculated to quantify the amount of variation over the whole set of input power values. A low standard deviation means the data are close to the mean value of the set, while a high standard deviation hints that the data are spread out over a wider range of values.

For a random variable vector A made up of N scalar observations, the standard deviation is defined as the square root of the variance, where μ is the mean of A:

$$S = \sqrt{\frac{1}{N-1}\sum_{i=1}^{N}|A_i - \mu|^2}$$
$$\mu = \frac{1}{N}\sum_{i=1}^{N} A_i \tag{6.7}$$

Calculate the standard deviation of input power over each period to observe its deviation from the average value. The commands in MATLAB are:

```
diff=(sign(Voltage(2:end))-sign(Voltage(1:end-1)))
num=find(diff==2)
P=zeros(1,9)
for  i=1:9
  P(i)=sum(Current(num(i):num(i+1)).*
  Voltage(num(i):num(i+1)))/(num(i+1)-num(i)+1)
end
std(P)
stdev = std(P)/mean(P) * 10^6
```


The results of standard deviation are illustrated in Table 6.9 and chart 6.20. There is no linear relationship between the input power deviation and the load resistance.

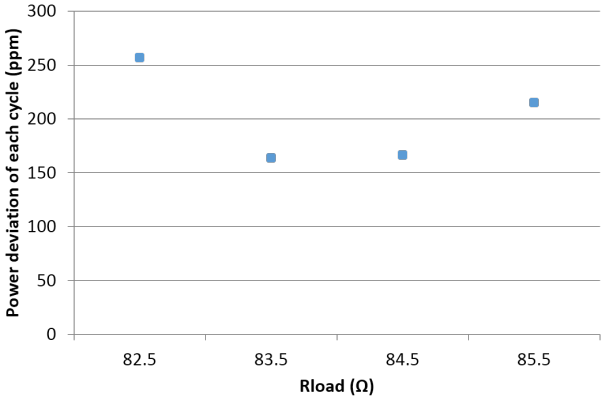

Figure 6.20: Standard deviation of input power deviation with change of load resistance

Table 6.9: Standard deviation of input power

R/Ω	82.5	83.5	84.5	85.5
STDEV/ppm	257.15	164.03	166.36	215.28

REFERENCES

[1] *News releases- ti introduces industry's first led controller with constant power regulation,* .

[2] Texas-Instruments, *Lm3447,* (), phase Dimmable, Primary Side Power Regulated, PFC Flyback Controller for LED Lighting.

[3] Texas-Instruments, *Using the lm3447-par-230vevm,* (), user's guide.

7

LINEAR REGULATORS AND SWITCHING MODE POWER SUPPLIES

So far, the input power of the transfer standard can be regulated at a constant level by using constant power controller LM3447. Apart from the electrical requirement at the input port, the transfer standard LED lamp should also meet optical demands at the output side. In consideration of light quality, the LED lamp should generate consistent luminous flux so that it is also a transfer standard with stable photometric parameters. As a result, LED loads need constant forward current, since the light output is proportional to the forward current.

The solution for constant output current is to insert another controller regulating the output current. The constant-current controller can be a switching mode power supply (SMPS) or a linear regulator (LR).

In this chapter, the basic operating principles, advantages and disadvantages, test results of both solutions are illustrated.

7.1. LINEAR REGULATORS AND SWITCHING MODE POWER SUPPLIES

In the power conversion process of delivering a regulated output voltage to the load side from an input source, low power loss and high energy efficiency are main concerns. Other considerations include light weight, small size and low cost. Both switching mode power supplies and linear regulators can achieve constant outputs, but they are applicable in specified situations depending on different performance requirements. Choosing between switching mode power supplies and linear regulators is important in power supply design.

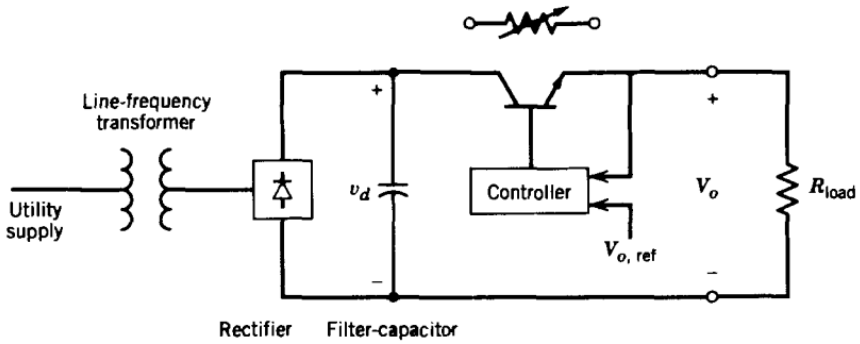

Figure 7.1: The direct current (dc) power supply to provide a regulated output voltage V_o to a load [1]. In the linear power supply, a line-frequency transformer is used to provide electrical isolation and for stepping down the line voltage. The rectifier converts the alternating current (ac) output of the thansformer low-voltage winding into dc. The filter capacitor reduces the ripple in the dc voltage v_d.

The objective of high efficiency is not easy to be achieved by linear regulators. A linear regular example is given in Figure 7.1, where the utility AC supply is converted to the DC power by a rectifier and then delivers a regulated output voltage V_o to the load.

In the linear regulator, the transistor is controlled by a output voltage feedback loop: the actual output voltage V_o is compared with the reference value $V_{o,\text{ref}}$, and the error determines the base current I_B. For the transistor, the collector-emitter voltage V_{CE} is decided by the base current I_B and is controlled to absorb the difference between V_d and V_o. The load current I_o goes through the transistor, so the transistor operating in the linear region behaves as a variable resistor V_{CE}/I_o. The power loss due to the heat in the transistor is the output current multiplied by the voltage difference. The efficiency can be estimated as:

$$\begin{aligned}\eta &= \frac{P_{\text{out}}}{P_{\text{out}} + P_{\text{loss}}} \\ &= \frac{V_o \cdot I_o}{V_o \cdot I_o + (V_{\text{in}} - V_o) \cdot I_o} \\ &= \frac{V_o}{V_{\text{in}}}\end{aligned} \tag{7.1}$$

The efficiency of the linear regulator is always low because of the power loss in the transistor, so the transistor needs enough thermal capacity and the linear regulator should have a large space to deal with the serious power dissipation problem. By the way, the efficiency of the linear regulator can be high only when V_o is very close to V_{in}.

Due to the collector-emitter voltage drop on the transistor, the input voltage of the power supply must be higher than the output voltage. In order to ensure the transistor to work in the linear region, a limitation on the minimum value of input-output voltage difference is always illustrated in the datasheet. Therefore, linear regulators can only be designed as step-down voltage regulators.

Even though linear regulators are low-efficient and can only realize voltage drop-down, they have advantages when it comes to simplicity and cost, but not efficiency. As a result, linear regulators can be applied in situations where the efficiency is not the main consideration, such as the transfer standard design in this project.

In contrast to linear regulators, switching mode power supplies (SMPS) are high efficient. Figure 7.2 shows an example of switching mode operation, in which the transistor works in switching mode instead of linear mode. When the transistor is turned on and current flows through it, the collector-emitter voltage drop is almost zero; when the transistor is off, there is almost no current goes through it. As a result, the transistor acts as an ideal switch and its power loss is minimized. The transistor switched on and off in high frequency has large switching loss, but its switching loss is normally rather lower than the power loss through the transistor in linear regulators.

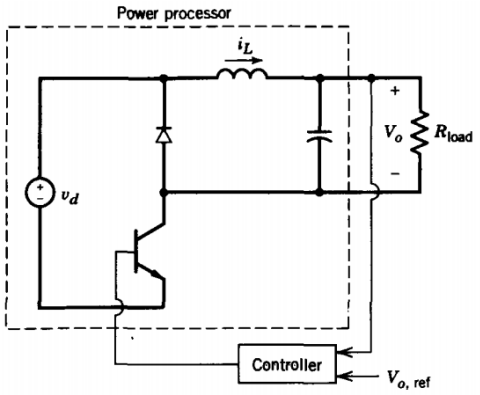

Figure 7.2: Switching mode power supply [1]. In power electronics, by operating the transistor as a switch at high switching frequency f_s, the dc voltage v_d is converter into an ac voltage at the switching frequency.

Since switching mode power supplies operate at very high frequencies, the components in the circuit, such as the transformer and the filter capacitor can be small and light compared with line-frequency components.

Another advantage of switching mode power supplies is that they can realize a variety of power conversion, such as buck, boost, buck-boost and inverting. This large flexibility in performing conversions brings more convenience to designers.

The disadvantage is switching mode power supplies require passive components such as inductors, capacitors and resistors. Therefore, the additional elements add complexity of the circuit. With regard to the cost of IC and complicated components, switching mode power supplies are normally more expensive than linear regulators.

7.2. TEST ON SWITCHING MODE POWER SUPPLIES

BECAUSE switching mode power supplies have higher efficiency and more flexibility in power conversion, a switching mode Buck driver RCD-48 using constant-current control is chosen to regulate the output current. The Buck LED driver has high-frequency

PWM control and is featured with high efficiency. In RCD-48 series, four values of output currents are available: 0.35 A, 0.5 A, 0.7 A and 1.2 A. In this LED driver design, 0.7 A output current is chosen based on the load requirement.

For the transfer standard LED driver design, it is impossible to regulate both the input power and the output current at a constant level by a single power converter. Under the constant output current, the output power changes with the LED resistance due to the temperature deviation, therefore, the law of conservation of energy is no longer obeyed in this circuit. In order to regulate both the input power and the output current at the same time, two cascaded converters are needed: one constant-power AC/DC converter LM3447 at the input side and the other constant-current DC/DC converter RCD-48 at the output side. A resistor is connected between those two converters so that the difference between the input power and the output power can dissipate through it. The topology is illustrated in Figure 7.3.

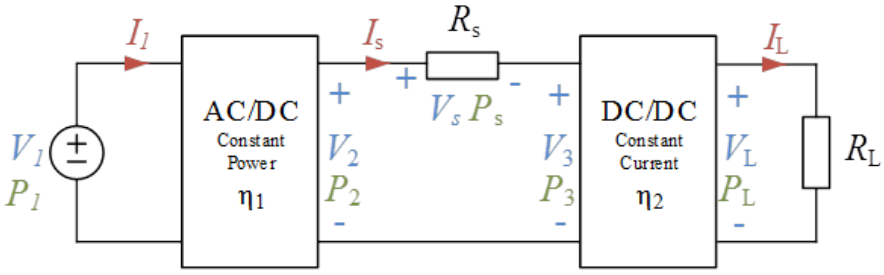

Figure 7.3: Switching mode converter solution. An AC/DC constant power controller is placed at the input side to regulate the input power. A DC/DC constant current converter is placed at the output side to achieve constant output current. A resistor R_s is connected between those two converters to absorb the energy difference between the input and the output.

In the schematic, the power P_s dissipated in the resistor R_s is the difference between the output power P_2 of LM3447 and the input power P_3 of RCD-48, and the relationship can be expressed into:

$$\begin{aligned} P_s &= P_2 - P_3 \\ I_s^2 \cdot R_s &= \eta_1 \cdot P_1 - \frac{P_3}{\eta_2} = \eta_1 \cdot P_1 - \frac{I_L^2 \cdot R_L}{\eta_2} \end{aligned} \tag{7.2}$$

The current through R_s is derived as:

$$I_s = \sqrt{\frac{\eta_1 \cdot P_1 - \dfrac{I_L^2 \cdot R_L}{\eta_2}}{R_s}} \tag{7.3}$$

As a result, the input voltage V_3 of RCD-48 can be related with the output current I_L as:

$$V_3 = \frac{P_3}{I_s} = \frac{\frac{I_L^2 \cdot R_L}{\eta_2}}{\sqrt{\frac{\eta_1 \cdot P_1 - \frac{I_L^2 \cdot R_L}{\eta_2}}{R_s}}} \tag{7.4}$$

On the other hand, the relationship between the input voltage V_3 and the output current I_L can also be measured. By gradually increasing V_3 and recording the corresponding I_L under various load resistance R_L, the output current results can be measured as shown in Figure 7.4.

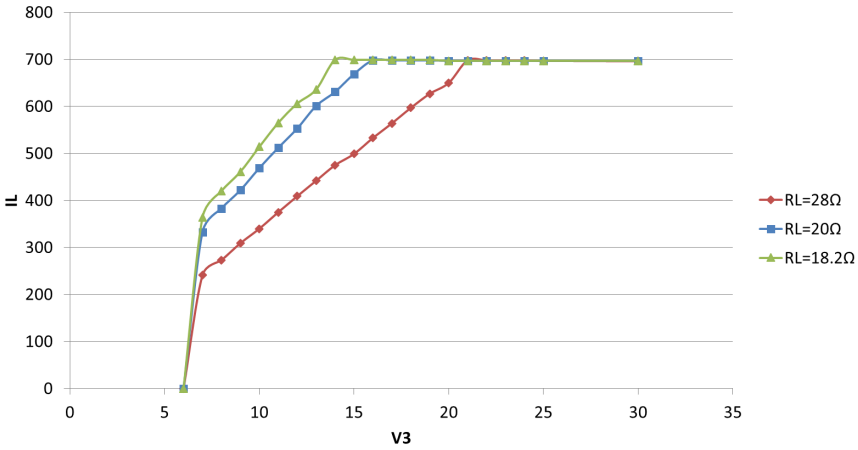

Figure 7.4: Output current measurement under various load resistance. When V_3 increases, the output current I_L first rises up and then keeps constant until V_3 reaches threshold value. The threshold value differs under various load resistance.

From the results, it can be observed that RCD-48 can not generate constant current all the time. The output current I_L begins to rise when V_3 is 6 V, and keeps increasing with V_3 rising. Until V_3 reaches a threshold value, I_L stays at a constant value 0.7 A, which is according to the specification of the converter. The input voltage threshold value increases with the load resistance rising. For example, under a 20 Ω load resistor, the input voltage threshold value is 16 V and the curve derived from measurement is shown in blue in Figure 7.5.

Another curve describing the relationship between the input voltage V_3 and the output current I_L can also be plotted based on Equation 7.4, see the red line in Figure 7.5. Two curves are plotted in one figure and their intersecting points are the operating points of the circuit. There are two intersecting points: the first intersection happens when V_3 is about 13 V and I_L is about 0.6 A; the second intersection happens when V_3 is about 21 V and I_L is about 0.7 A. The second point is the expected operating point, because at that point the output current is at its rated value 0.7 A.

In the next step, do experiment on the circuit to find the operating points in real situation. The actual operating point happens when V_3 is 12.8 V and I_L is 0.57 A, the point which is very close to the first intersection in Figure 7.5. At this operating point, the input voltage of RCD-48 has not reached the threshold value 16 V so that the output current can not keep at a rated value 0.7 A.

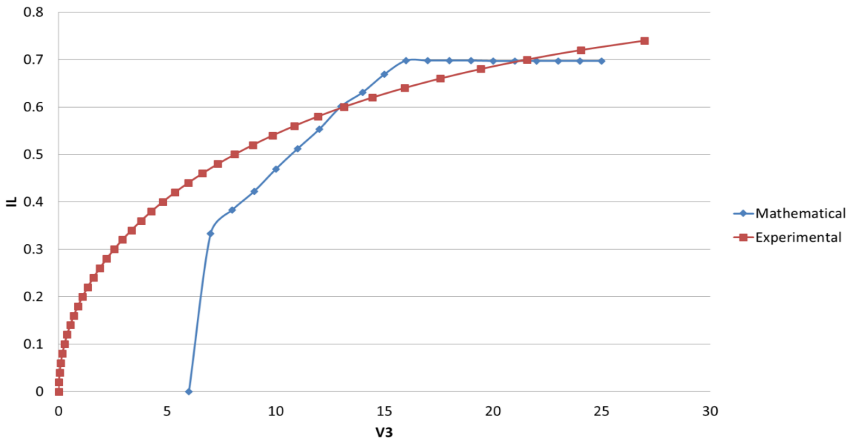

Figure 7.5: Relationship between I_L and V_3 under 20 Ω load. The blue curve is the experimental results of I_L and V_3 measured before. The red curve is plotted from the mathematical equation illustrated in Equation 7.4. The intersections of those two curves are the operating points in the circuit.

The test results show that it is impossible to reach the expected operating point whose output current is at the rated constant value, because V_3 and I_L stop rising to higher values any more as long as they reach a intersection point at a lower level. As a result, using switching mode controller RCD-48 can not achieve constant-current output.

7.3. TEST ON LINEAR REGULATORS

SINCE the switching mode converter RCD-48 fails to realize constant-current output, another solution of linear regulators has been conducted. A three-terminal linear regulator LM317 that can supply constant output current is applied to the circuit. The functional block diagram of LM317 is given in Figure 7.6.

The NPN Darlington transistor output topology is made up of two bipolar transistors in the way that the emitter of one transistor is connected to the base of the other one. This structure can generate a quite larger current gain which is the product value of current gains of two separated transistors, so only a small amount of base current is needed to turn on the transistor. The collector-emitter voltage across the NPN Darlington transistor absorbs the voltage difference between INPUT and OUTPUT.

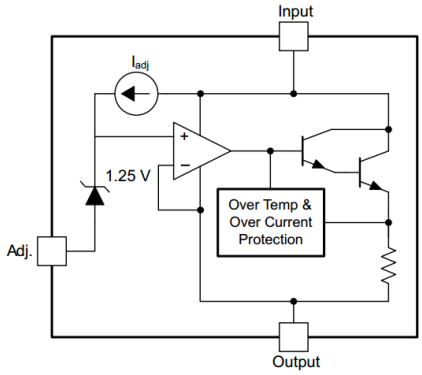

Figure 7.6: Functional block diagram [2].The LM317 has three terminals: input, output and adjust. The zener diode at the non-inverting input of the amplifier provides 1.25 V breakdown voltage. Through the feedback control loop, the amplifier with 1.25 V offset is capable of keeping OUTPUT voltage 1.25 V higher than ADJUST voltage.

For current application, a resistor R_s is connected between terminal OUTPUT and ADJUST whose resistance is selected based on the output current requirement. The output current can be regulated to $1.25/R_s$, since the current flowing through ADJUST is negligible. In the example of constant-current battery-charger circuit in Figure 7.7a, the battery is charged at a constant current $I_{\text{CHG}} = 1.25/R_s$. Considering the input-to-output voltage difference, V_{IN} should be greater than $V_{\text{BAT}} + 1.25V\,[V_{\text{REF}}] + 3V\,[\text{headroom}]$.

For voltage application shown in Figure 7.7b, a series resistor R_s restricts the output current of the LM317, and two resistors R_1 and R_2 regulate the output voltage to $\left(1+\frac{R_2}{R_1}\right)\cdot 1.25$.

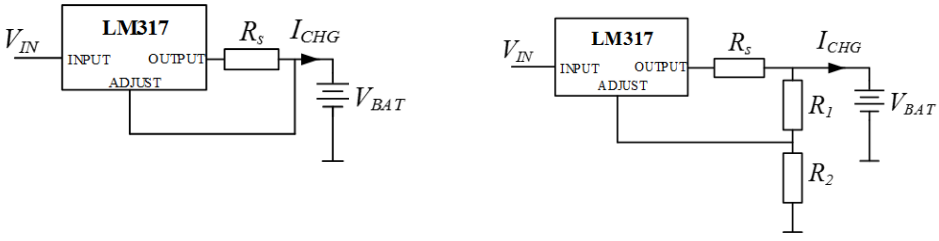

(a) (b)

Figure 7.7: (a) Current application of LM317. The R_s connected between OUTPUT and ADJUST terminal can regulate a constant output current to the battery. (b) Voltage application of LM317. The R_1 and R_2 are used to set a constant output voltage to the battery.

To investigate the operation of LM317 as a voltage regulator, build a circuit as shown in Figure 7.8. Two resistors R_{fbt} and R_{fbb} are used to set the output voltage V_o:

$$V_o = \left(1 + \frac{R_{\text{fbb}}}{R_{\text{fbt}}}\right) \cdot V_{\text{ref}} = \left(1 + \frac{698}{237}\right) \cdot 1.25 = 4.93V \tag{7.5}$$

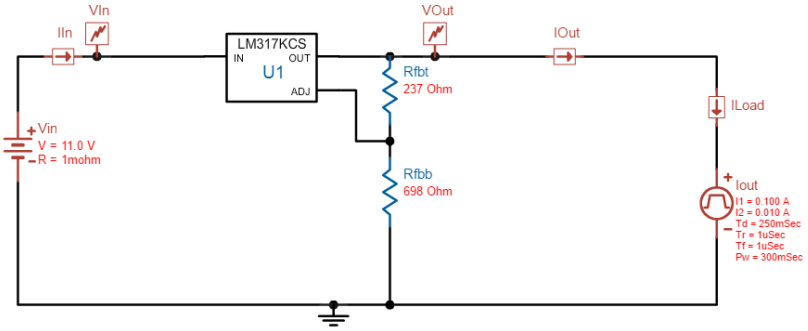

Figure 7.8: Simulation circuit for load regulation. The load current is changed from 0.1 A to 0.01 A. Whether the output voltage can keep constant is checked.

The line transition in Figure 7.9a shows that when the input voltage (in blue) steps from 10 V to 12 V, the output voltage (in red) changes from 4.971 V to 4.972 V, achieving about 0.02 % line regulation. The load transition in Figure 7.9b shows that when the output current changes from 0.1 A to 0.01 A, the output voltage (in red) keeps stable, achieving good load regulation. The simulation proves that the LM317 can realize voltage regulation via two resistors and its inner feedback control scheme.

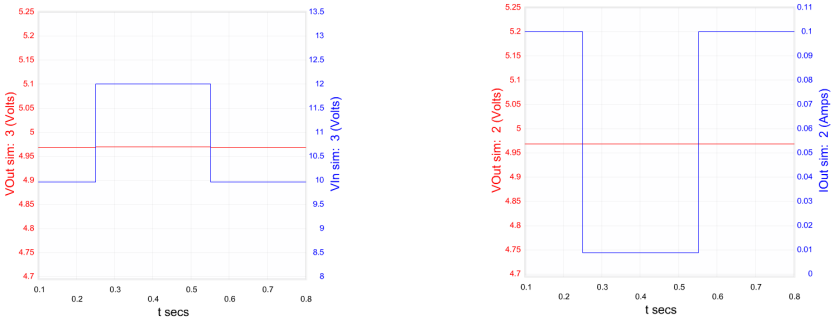

(a) (b)

Figure 7.9: Results of transient simulations on LM317. (a) Input transition: The output voltage keeps constant when the input voltage has a step change. (b) Load transition: the output voltage keeps constant when the load current is changed.

Since the LM317 can achieve a reliable constant-current output, this linear regulator can be applied in the transfer standard driver circuit. The circuit is designed as shown in Figure 7.10.

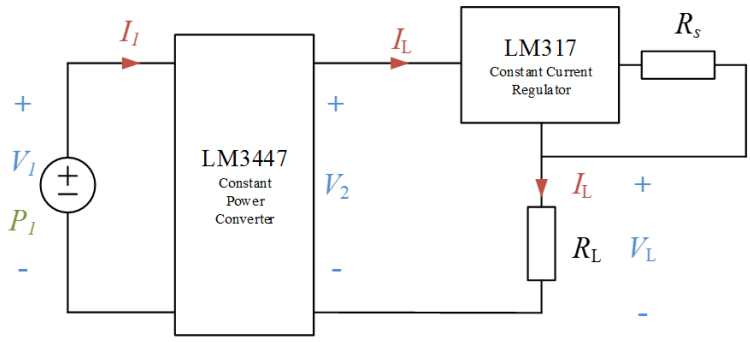

Figure 7.10: Linear regulator solution. A constant power converter LM3447 is placed at the input side to regulate the input power. A constant current regulator LM317 used to control the output current.

From the protection test on LM3447, it has been known that its load resistance should be lower than 86 Ω to prevent open circuit protection and be higher than 19.8 Ω to prevent short circuit protection. Since the output voltage of LM3447 is measured as around 35 V, the minimum and maximum output current of LM3447 is:

$$\begin{aligned} I_{\text{L,min}} &= V_{\text{out}} / R_{\text{max}} = 35/86 = 406.98\text{mA} \\ I_{\text{L,max}} &= V_{\text{out}} / R_{\text{min}} = 35/19.8 = 1.767\text{A} \end{aligned} \tag{7.6}$$

Because the output current requirement of LM317 is the same as the output current of LM3447, and the reference voltage between OUTPUT and ADJUST terminal is 1.25 V, the maximum and minimum value of R_s is:

$$\begin{aligned} R_{\text{s,max}} &= V_{\text{ref}} / I_{\text{L,min}} = 1.25/0.406 = 3.07\Omega \\ R_{\text{s,min}} &= V_{\text{ref}} / I_{\text{L,max}} = 1.25/1.767 = 0.707\Omega \end{aligned} \tag{7.7}$$

Therefore, the series resistor R_s is selected as 2 Ω, connected between OUTPUT and ADJUST terminal of LM317. It regulates the load current I_L to 625 mA.

REFERENCES

[1] N. Mohan and T. M. Undeland, *Power electronics: converters, applications, and design* (John Wiley & Sons, 2007).

[2] Texas-Instruments, *Ulm317 3-terminal adjustable regulator,* .

8

OVERALL TEST ON TRANSFER STANDARD

8.1. TRANSFER STANDARD TOPOLOGY

BY far, the transfer standard driver topology has been determined and proved feasible. In the real application of the transfer standard, the load is a series of LEDs instead of resistors. Therefore, to complete the whole design, the load resistor is replaced with the LEDs and the circuit is given in Figure 8.1. The input of the constant power converter LM3447 is connected to the AC power supply, and its output is connected to the constant current regulator LM317 and LED loads. The LM317 series resistor R_s is set to 2 Ω. The LM317 together with LEDs can be considered the load of the LM3447.

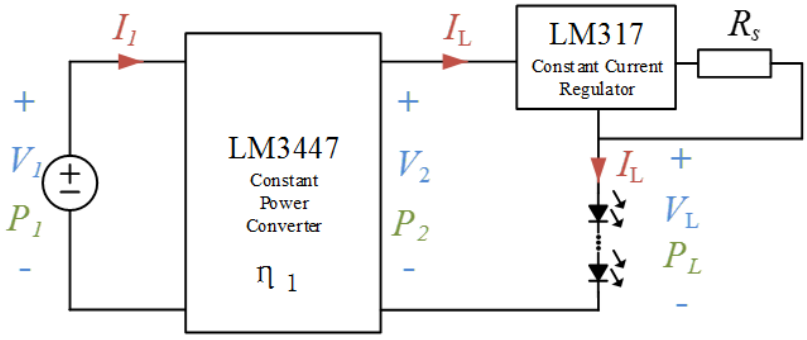

Figure 8.1: The final topology for the transfer standard LED lamp. The constant power converter LM3447 is connected at the input side to regulate the input power. The constant current regulator is placed at the output side to maintain a constant output current. Several LEDs are used as loads.

The numbers of LEDs are adjusted and the load currents are measured, as listed in Table 8.1. When ten LEDs are used as loads, the 500 mA load current is much lower than

the rated load current 625 mA. The input voltage V_2 and the output voltage V_L of LM317 is measured as 32.09 V and 29.88 V, so the differential voltage is $32.09-29.88=2.21V$. Since LM317 needs a minimum of 3 V differential voltage to operate in the linear region, the 2.21 V differential voltage can not support its normal operation so that the load current is far from its rated value. Similarly, when eight LEDs are connected, the 598 mA load current is lower than the rated value.

Under seven LEDs, the differential voltage is about 5 V, so the transistor in the LM317 is able to work in the linear region and the load current can be kept at 632 mA. Therefore, the load is determined to be seven LEDs. The forward voltage is approximately 21 V and the forward current is about 632 mA.

Table 8.1: Investigation on numbers of LEDs

Numbers	I_L/mA	V_2/V	V_L/V
10 × LEDs	500	32.09	29.88
8 × LEDs	598	27.15	24.46
7 × LEDs	632	26.28	21.02

8.2. TEST ON TRANSFER STANDARD

8.2.1. TEST ON THE FIRST PROTOTYPE

Build the transfer standard driver circuit based on the schematic shown in Figure 8.1. Measure the load current I_L, the load voltage V_L, the output voltage of LM3447 V_2 by multimeters. Record the input power P_{in} by the Digitizer. The measurement results are illustrated in Table 8.2. The first set of data is recorded when the power supply is just turned on and the temperature is still low. As the LEDs emit the light, the temperature begins rising so that operating points changes until the system becomes stable. The second set of data is the results at final state.

Table 8.2: Test on the first prototype

	I_L/mA	V_L/V	V_2/V	P_{in} /W	R_L/Ω	R_2/Ω
1	628	21.11	26.39	19.04	33.61	42.02
2	632	20.58	26.11	18.86	32.56	41.31
pct.	0.64 %	2.51 %	1.06 %	0.94 %	3.13 %	1.69 %

It can be observed that I_L is not constant, rising from 628 mA to 632 mA with about 0.64 % change. The reason is that the LM317 series resistance R_s may change due to the temperature increasing, since the resistor has a high temperature coefficient.

With the temperature rising and the load resistance R_L changing 3.13 %, thanks to the constant-power converter LM3447 and the linear regulator LM317, the variation of the input power P_{in} is restricted to 0.94 % and the fluctuation of the load current is only 0.64 %. In contrast, the input power variation is estimated to be 3.13 % if using a constant-current driver. Therefore, this transfer standard can regulate both the input power and the load current at the same time, so that it performs better than the constant-current driver when applied in test laboratories.

8.2.2. TEST ON THE PROTOTYPE WITH A NEW SERIES RESISTOR

In order to improve the stability of the load current, the LM317 series resistor is replaced with a power resistor which is less sensitive to temperature deviation. Also, this resistor is placed on the heatsink for better thermal dissipation. Therefore, the new power resistor is featured with more stable resistance as temperature changes so that it is expected to regulate the load current better. Do the same measurements as described before and record the results in Table 8.3.

The results show that the load current variation reduces to 0.32 %, rather smaller than before, since the power resistor fluctuates little with the temperature and thus well regulating the load current. The load current is a little different from the value in the previous test, because the series resistance may not be exactly the same even though two resistors are both labelled 2 Ω.

What's more, the input power variation is limited to 0.95 % when the load resistance changes 2.67 %. Even though the input power variation has already been well regulated, the factors influencing the variation need to be found out and eliminated for more precise regulation.

Table 8.3: Test on the prototype with a new series resistor

	I_L/mA	V_L/V	V_2/V	P_{in} /W	R_L/Ω	R_2/Ω
1	624	21.19	26.52	18.99	33.96	42.50
2	622	20.56	26.46	18.81	33.05	42.54
pct.	0.32 %	2.97 %	0.23 %	0.95 %	2.67 %	0.09 %

8.2.3. TEST ON THE PROTOTYPE WITH FAN COOLING

To further improve the input power regulation, use the fan to cool down the LM3447 evaluation board so as to eliminate the temperature influence on it. The temperature deviation mostly influence the LM3447 because the characteristics of LM3447 pin voltages and internal control voltages are dependent on the temperature, according to the LM3447 datasheet. For example, V_{REF} changing with the temperature will influence the error amplifier and the PWM comparator in LM3447, and thus causing uncertainties in the input power regulation.

Table 8.4: Test on the prototype with fan cooling

	I_L/mA	V_L/V	V_2/V	P_{in} /W	R_L/Ω	R_2/Ω
1	624	21.19	26.52	18.99	33.96	42.50
2	622.5	20.56	26.57	18.95	33.03	42.68
pct.	0.24 %	2.97 %	0.19 %	0.21 %	2.74 %	0.43 %

Table 8.4 shows the test results of the prototype with fan cooling. The first set of data is recorded when the power supply is just turned on and the temperature is still low.; the second set of data is the final state after the fan cooling down the LM3447.

By enforcing the temperature on LM3447 to the original value, the input power variation can be limited to only 0.21% with the load resistance changing 2.74%. Even though

the LED resistance R_L changes 2.74 % with the temperature rising, the LM3447 equivalent output resistance R_2 deviates only 0.43 %. According to the test on LM3447 in Section 6.6, LM3447 is able to regulate a stable input power as the load resistance changing about 2 %. Therefore, the 0.42 % load resistance fluctuation makes almost no disturbance on the input power.

On the other hand, the output current variation is regulated to 0.24 %, so the transfer standard driver is able to regulate the LED current at a constant level and thus generating consistent luminous flux for optical measurement. The precision of the output current can be further improved by using a highly stable series resistor for LM317.

8.3. COMPARISON OF THREE TRANSFER STANDARDS

SINCE different driver topologies and ambient temperature can lead to different measurement results of the input power, the input power variation is measured under three transfer standards: the first one is a commercial LED lamp; the second one is the transfer standard without fan cooling; and the third one is the transfer standard with fan cooling. The results of input power changing with time are plotted in Figure 8.2, in which the input power values are normalized for easy comparison between different transfer standards. Input power variation within 0.5 % is the requirement for the standard scenario in test laboratories and 0.2 % is for the stringent scenario. 0.1 % input power variation is the ultimate goal of this project. The results of input power variation and rms current variation of three transfer standards are listed in Table 8.5 and the time for stabilization are illustrated in Table 8.6.

It can be inferred from Table 8.5 that the transfer standard with fan has the smallest variation in input power, rms current and power factor, while the commercial LED lamp has the largest variation in them. Therefore, the transfer standard with fan has a stable performance as an electrical load. Its power factor value is about 0.96, close to unity, while the power factor value of the LED lamp is lower, about 0.82.

Table 8.5: Comparison of input power variation, rms current and power factor (PF)

	Δ P	ΔI_{rms}	Δ PF
lamp	3.66 %	7.06 %	1.14 %
without fan	1.63 %	1.96 %	0.29 %
with fan	0.49 %	0.64 %	0.10 %

Table 8.6: Comparison of time reaching stability according to different input power variation ranges

	0.5 %	0.2 %	0.1 %
lamp	25 : 05	34 : 17	44 : 37
without fan	05 : 14	11 : 54	18 : 13
with fan	instant	01 : 38	03 : 24

It can be observed in Figure 8.2 that three input power curves all drop down from

an initially high level and after some time they gradually enter a stable level. However, the time before stability and the degree of variation are different between three transfer standards.

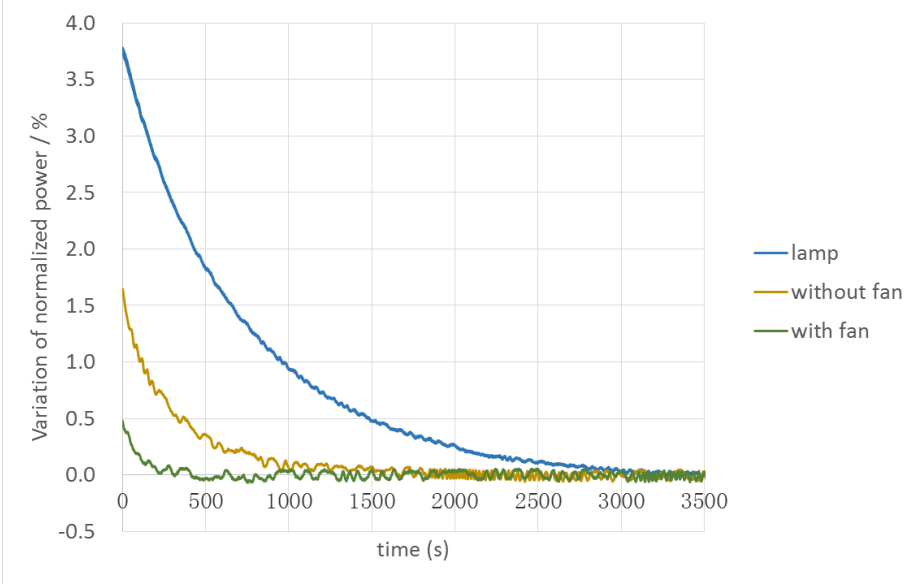

Figure 8.2: Comparison of input power variation of three transfer standards. Three input power curves drop down from an initially high level and gradually enter a stable level after some time. For the commercial LED lamp, the input power variation of 3.66 % is the largest among three and the stabilization time of 25 minutes is the longest. For the transfer standard with fan cooling, the power variation of 1.63 % is the smallest and the stabilization time is the shortest.

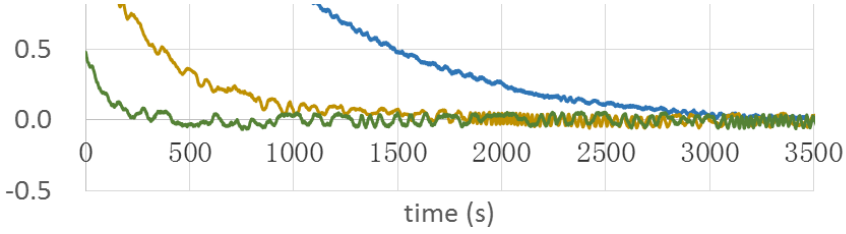

Figure 8.3: Zoom-in figure of the input power variation comparison

For the commercial LED lamp, its input power variation of 3.66 % is very large and it takes over 25 minutes to reach stabilization for standard scenario measurement. This large variation and long stabilization time lead to large measurement errors and unreliable measurement results. If test laboratories use the commercial LED lamp as the transfer standard, the inconsistency of measurement results will cause problems in determining LED products specifications. Therefore, the commercial LED lamp is unsuit-

able for test laboratories.

In comparison, the transfer standard without fan cooling has a relatively low input power variation of 1.63 % and a shorter time for stabilization, as shown in the yellow line. It only takes about 5 minutes to reach 0.5 % requirement of the standard scenario. Featured with relatively low variation and rapid stabilization, the transfer standard without fan cooling can be a good candidate for the measurement tool used in text laboratories.

Furthermore, the transfer standard with fan cooling has the smallest input power variation of 0.49 % so that it can meet the 0.5 % demands of the standard scenario instantly after turning on. Even though it achieve the aim of 0.1 % instantly after turning on, it keeps fluctuating within 0.1 % after a short warm-up time of 3.5 minutes. As a result, the transfer standard with fan cooling has the lowest power variation and the most rapid stabilization.

Therefore, the transfer standard that applies the proposed driver topology and keeps the temperature of LM3447 stable can achieve accurate input power measurement results and realize rapid stabilization, so that it can be applied to check measurement setups in test laboratories.

9

DUMMY LOAD DESIGN

As mentioned before, there are two potential solutions of the transfer standard LED lamp: a Flyback converter with an optical load and a dummy load with no optical output. By far, the power electronics converter design has been carried out and proved feasible. Furthermore, another solution of the dummy load has also been conducted in this project.

The dummy load device behaves like a reliable standard power reference source because it can simulate the feature of SSL products, including the voltage and current waveforms. It is able to establish traceability of measurement results and to provide highly accurate calibration for measurement setups in test laboratories.

9.1. DUMMY LOAD DESIGN

The block diagram of the dummy load device is shown in Figure 9.1. The dummy load power standard includes a Raspberry Pi (RPI), an arbitrary waveform generator AFG1062, a voltage amplifier and a transconductance amplifier. The outputs of the power standard in connected to a power meter, which is the measurement setup under validation in test laboratories.

The Raspberry Pi operates as an upper computer to control the arbitrary waveform generator AFG1062 in the way of commanding the mode switching and initialization of each test mode. AFG have two output channels: a current channel (CH1) and a voltage channel (CH2), and its output amplitude is ranged up to 10 V_p. Predefined voltage and current waveforms can be directly programmed into AFG1062 through an external USB memory stick by ArbExpress software. The current and voltage waveforms generated from AFG1062 are respectively sent to the transconductance amplifier and the voltage amplifier.

An incandescent lamp is simulated by two sinusoidal waveforms representing its voltage and current, as shown in Figure 9.2. Furthermore, the incandescent lamp with a dimmer is represented by two cut-off waveforms as Figure 9.3 shows. The dimming incandescent lamp behaves as a nonlinear load which generated rich harmonics in voltage and current waveforms.

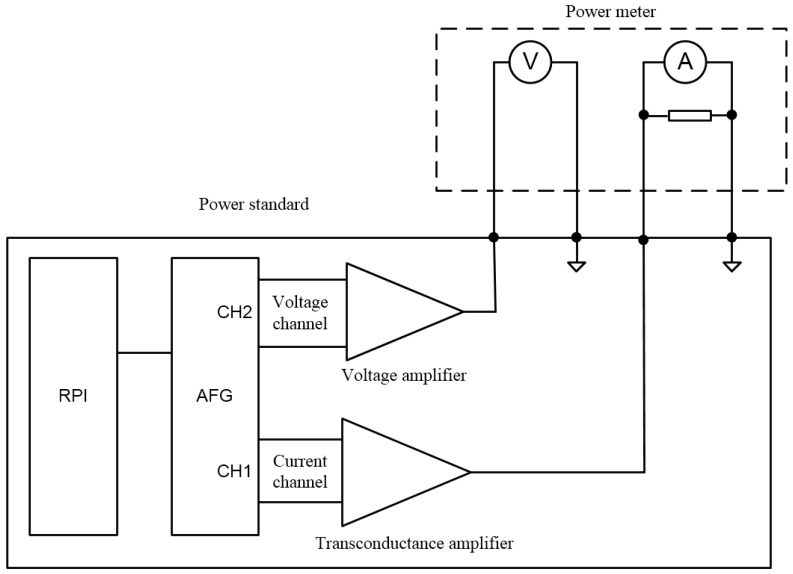

Figure 9.1: Diagram of the standard power reference source. The dummy load power standard includes a Raspberry Pi (RPI), an arbitrary waveform generator AFG1062, a voltage amplifier and a transconductance amplifier. The voltage output of the power standard is connected to the voltage meter and the current output is connected to the current meter.

To investigate the real lighting products, eight solid-state lighting (SSL) lamps are replicated by a sinusoidal voltage waveform and different shapes of current waveforms depending on the lamp driver. The current waveforms of these selected SSL lamps are previously recorded. Models of the selected SSL lamps are listed in Table 9.1 and their waveforms are shown in Figure 9.4. Each waveform is sampled in a sampling rate of 500 kSa/s and saved as 10k points with 24-bit magnitude resolution. Theoretically, information of harmonics up to 250 kHz can be reproduced.

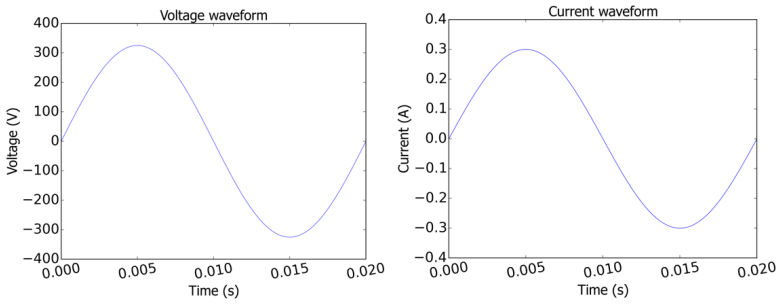

Figure 9.2: Voltage and current waveforms of replicating an incandescent lamp

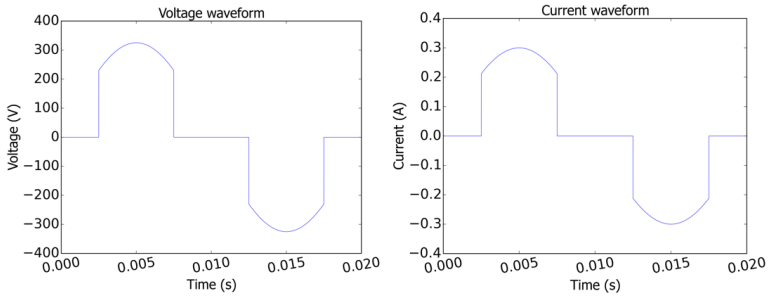

Figure 9.3: Voltage and current waveforms of replicating a non-linear load

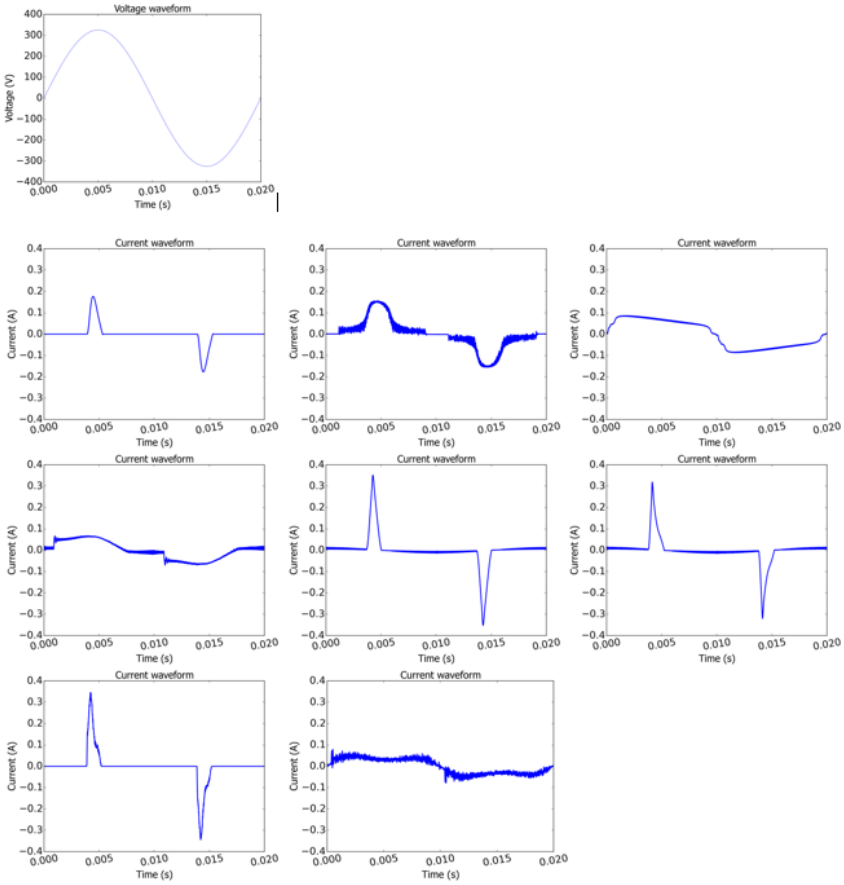

Figure 9.4: Voltage and current waveforms of replicating Lamp L01, L02, L04, L05, L06, L07, L08 and L11

Table 9.1: Models of the selected SSL lamps for replicating

Lamp	Model
L01	OSRAM PARATHOM PAR16 20
L02	Philips MASTER LED bulb MV
L04	Osram: Parathom A80
L05	Osram: Parathom A40FR
L06	Atlas E27 Warm white 3000K 6.6 W 380 lm IP20
L07	Energetic Warm white, 6 W, >250 lumen
L08	Home Lights E27 6.5 W 260 lm 3000K
L11	Verbatim 230-9573 Warm white E27 7.7 W

9.2. TEST ON VOLTAGE AMPLIFIER

THE arbitrary waveform generator AFG1062 generates a 9.3 V_p sinusoidal voltage waveform and delivers it to the voltage amplifier. The gain of the voltage amplifier is designed to be 35, in order to achieve a 325 V_p (230 V_{rms}) sinusoidal voltage waveform. The voltage amplifier is built using Apex Microtechnology PA94, a MOSFET power operational amplifier. PA94 is featured with a high slew rate of 500 V/μs.

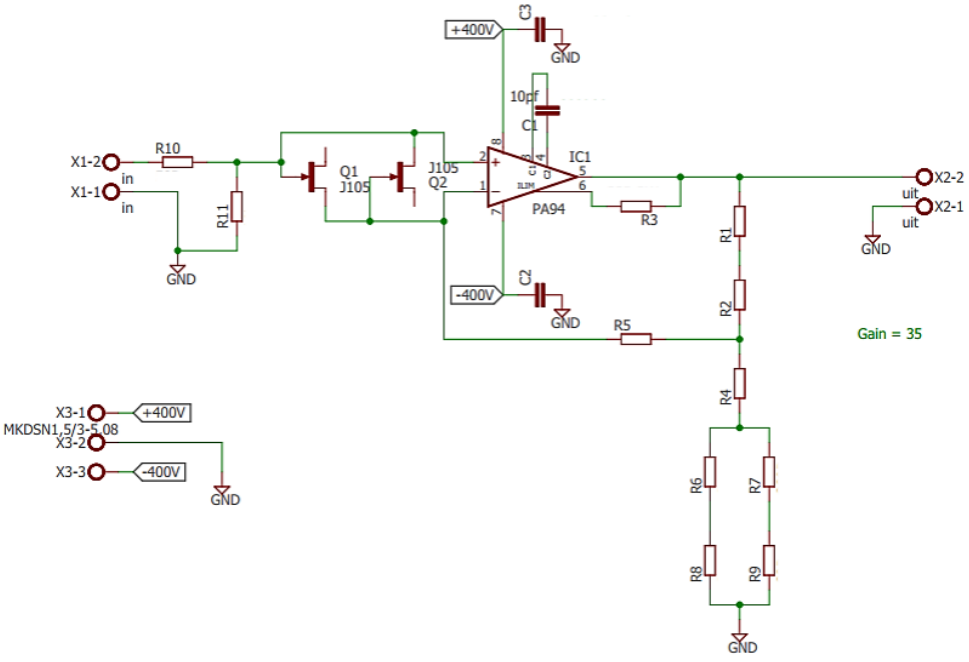

Figure 9.5: Schematic of the voltage amplifier. The schematic is built using a MOSFET power operational amplifier PA94. The resistors R_1 to R_9 in the feedback loop are used to set the amplifier gain.

The schematic of the voltage amplifier is shown in Figure 9.5. The amplifier gain is set by selecting proper resistance in the feedback loop.

Test the voltage amplifier by connecting its input to the voltage channel output of AFG1062. Record the input and output voltage waveforms of the voltage amplifier under different frequencies by the oscilloscope. The measurement results are shown in Figure 9.6.

In Figure 9.6a, when the frequency is 50 Hz, the sinusoidal waveform generated by AFG1062 is displayed in yellow (CH1), and its peak-to-peak value is 10.6 V as measured through the oscilloscope. The output voltage after amplification is shown in blue (CH2) and its peak-to-peak value is 3.6 V. Since the attenuation of CH2 is 1:100, the gain of voltage amplifier under 50 Hz is $3.6 \times 100/10.6 = 34$.

Similarly, measure the input and output voltage waveforms of the voltage amplifier under 1 kHz, 50 kHz and 200 kHz. The voltage waveforms are shown in Figure 9.6. Peak-to-peak values of CH1 and CH2, and RMS values of CH2 are measured by the oscilloscope and recorded in Table 9.2. RMS values of CH2 are calculated from their peak-to-peak values. Gains under different frequencies are derived using peak-to-peak values of input and output voltages.

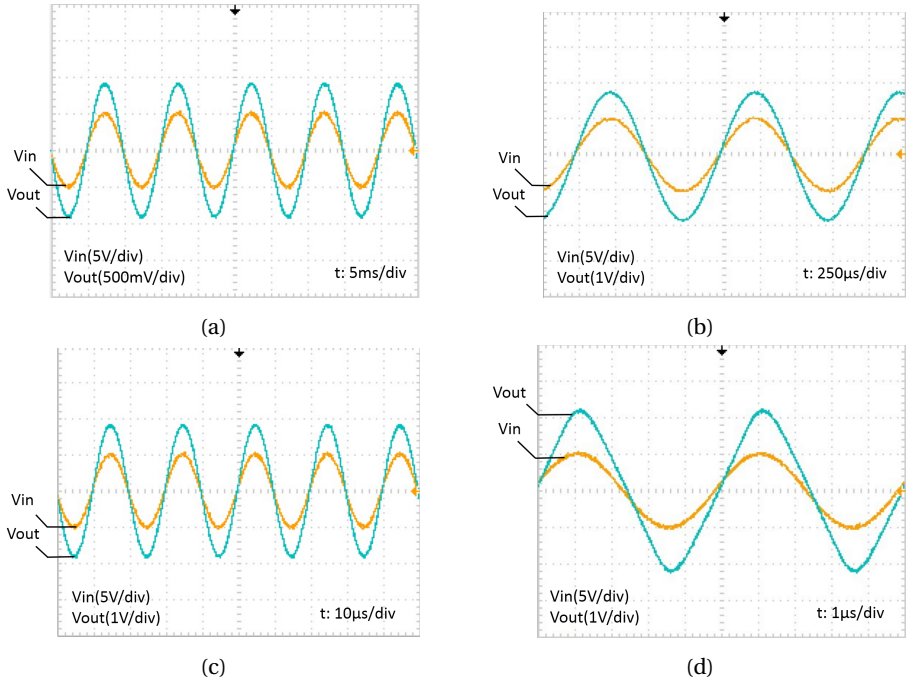

Figure 9.6: Input and output signal waveforms of voltage amplifier at different frequencies. (a) 50 Hz. (b) 1 kHz. (c) 50 kHz. (d) 200 kHz. When the frequency is below 200 kHz,

It can be analyzed from Figure 9.6 that under the frequencies of 50 Hz, 1 kHz and 50 kHz, the output waveforms of the voltage amplifier are all sinusoidal and the crest factors

are calculated. For a sinusoidal waveform, the crest factor should be 1.414. That means no distortion during voltage amplification under those frequencies. The amplifier gains are close to the expected value 35. The deviation is probably due to the limited precision of the oscilloscope.

However, when the frequency is 200 kHz, the output waveform of the voltage amplifier is roughly triangular waveform, instead of sinusoidal waves. It can be observed from Figure 9.6d that the slope of the output voltage waveform is 224 V/μs. The maximum slew rate of PA94 obtained from the assembled voltage amplifier is 224 V/μs and this maximum value is rather lower than 500 V/μs claimed in PA94 datasheet.

What's more, the amplifier gain is 41.5 under 200 kHz, far away from the designed value 35. Figure 9.7 shows the frequency dependence of the voltage amplifier gain. The amplifier gain can normally be 35 when frequencies are below 200 kHz. However, the gain will differ from the normal value if the frequency is over 200 kHz because the slew rate exceeds to the limitation of PA94.

The upper frequency range can be doubled with the level of the input signal reduced by half. For 5 V input signal, the upper frequency limitation is 200 kHz; for 2.5 V input voltage, the maximum frequency can reach 400 kHz.

Table 9.2: Input and output results of voltage amplifier under various frequencies

f / Hz	V_{P1} / V	V_{P2} / V	Gain
50	10.6	360	33.9
1 k	10.8	368	34.1
50 k	10.8	376	34.8
200 k	10.8	448	41.5

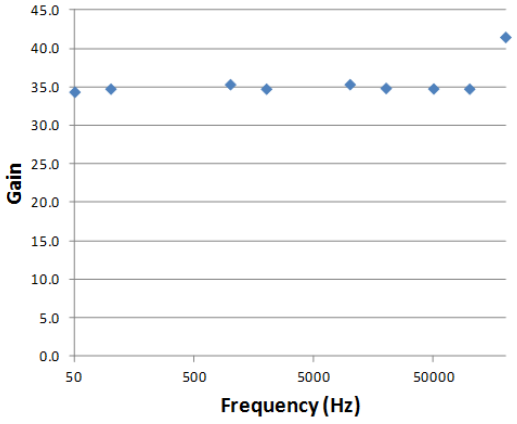

Figure 9.7: The frequency dependence of the gain of the voltage amplifier. The amplifier gains are about 35 when frequencies are below 200 kHz. However, when the frequency is over 200 kHz, the gain will deviate from 35.

9.3. TEST ON TRANSCONDUCTANCE AMPLIFIER

THE arbitrary waveform generator AFG1062 generates a 0.3 V_p sinusoidal voltage waveform and delivers it to the transconductance amplifier. The gain of the transconductance amplifier is designed to be 1 A/1 V. The transconductance amplifier is built using PA02A, a wide-band, high output current operational amplifier. It features high bandwidth of 350 kHz, high slew rate of 20 V/μs and high output current of ±5 A peak value. The schematic of the transconductance amplifier is shown in Figure 9.8.

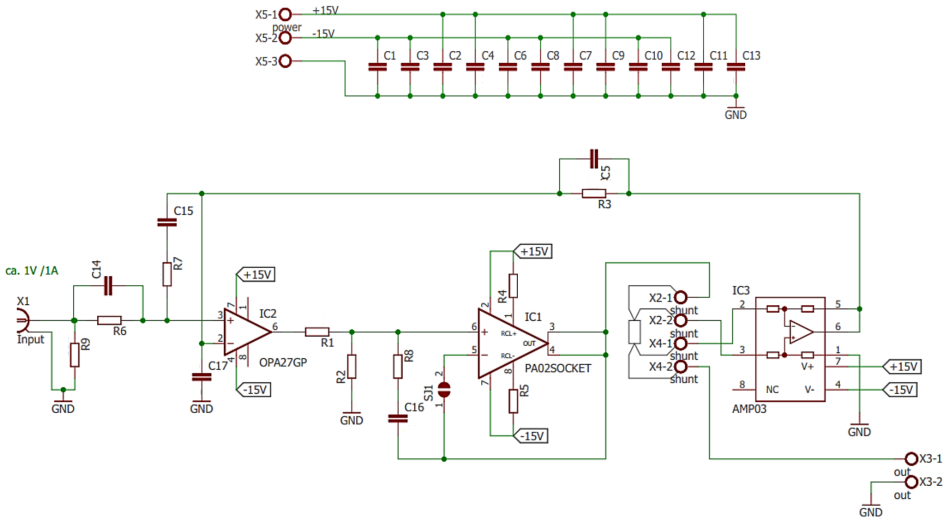

Figure 9.8: Schematic of transconductance amplifier. The schematic is built using a power operational amplifier PA02.

Since current waveforms of non-linear SSL products normally have rich harmonics at high frequencies, the bandwidth of the transconductance amplifier should be large enough to prevent current waveforms from distortion. The input and output signal waveforms are measured at different frequencies and recorded in Figure 9.9.

Under frequencies 50 Hz, 1 kHz and 20 kHz, the input voltages of the transconductance amplifier (CH1, in yellow) are sinusoidal waveforms with a 0.3 V_p. The output voltage (CH2, in blue) are also sinusoidal waveforms, with a 3 V peak-to-peak value and are almost overlapped with input voltages. The conversion factor of CH2 is 10 V/1 A, so the peak-to-peak value of the output current is 0.3 A, achieving 1 A/1 V transconductance amplifier gain.

When the frequency increases to 100 kHz, the output waveform has distortion so it is no longer sinusoidal, as shown in Figure 9.9d. Furthermore, as the frequency increases, the output distortion becomes rather obvious so that the output waveforms become triangular waves instead of sine waves, as shown in Figure 9.9e and Figure 9.9f.

In conclusion, the bandwidth of the assembled transconductance amplifier is 100 kHz. Since the peak of current harmonics appears around 40 kHz as proved in Section

3.1.2, the 100 kHz bandwidth of the assembled current amplifier can ensure the fidelity of current waveforms.

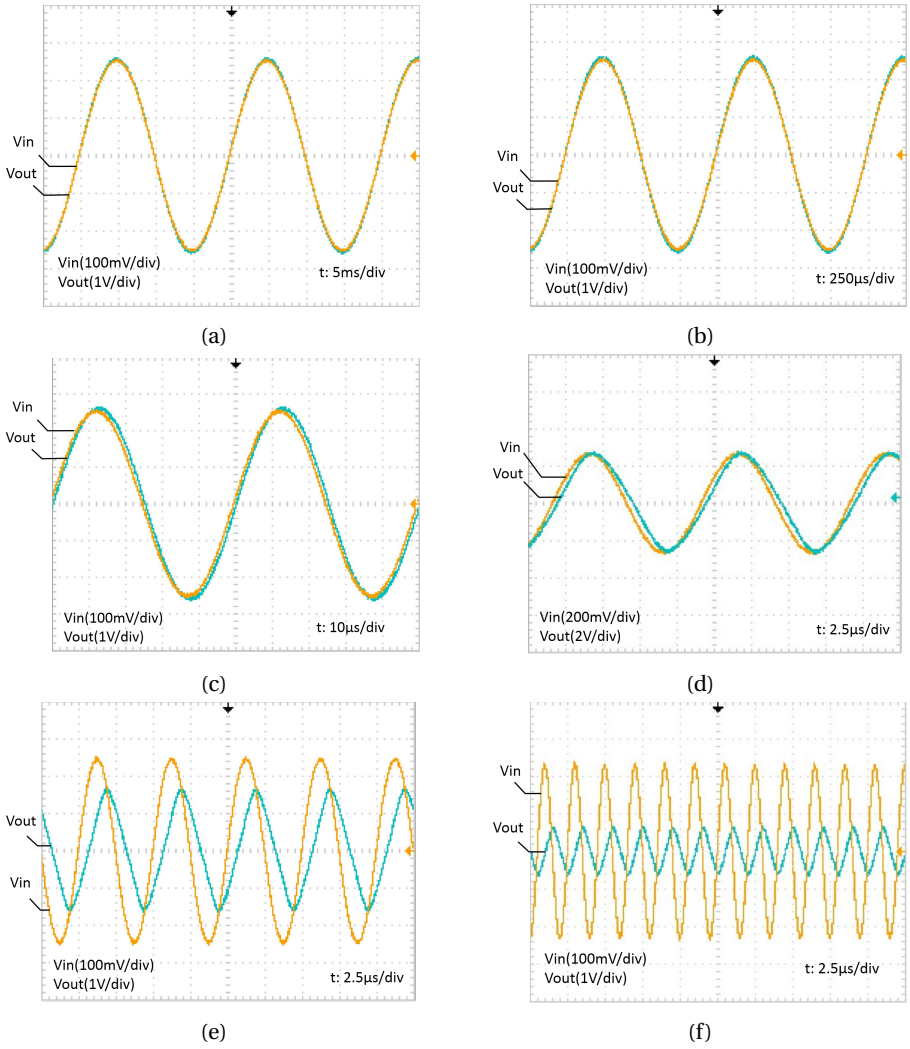

Figure 9.9: Input and output signal waveforms of transconductance amplifier at different frequencies. (a) 50 Hz. (b) 1 kHz. (c) 20 kHz. When the frequency is below 20 kHz, the output waveform is sinusoidal. (d) 100 kHz. When the frequency reaches 100 kHz, the output waveform transfers from sinusoidal to triangular. (e) 200 kHz. (f) 500 kHz. As the frequency increases, the output waveforms are distorted and become totally triangular.

9.4. COMPLETE ASSEMBLY

THE complete assembly of the dummy load power standard is shown in Figure 9.10, in which the voltage amplifier and the transconductance amplifier are assembled

in, as shown in Figure 9.11 and Figure 9.12. The Raspberry Pi provides the user interface to select the corresponding SSL lamp for simulating. Buttons from left to right are used to select the previous and select the next, turn on and turn off the output and shutdown the control unit. The user interface of Raspberry Pi when starting and selecting the waveform are shown in Figure 9.13.

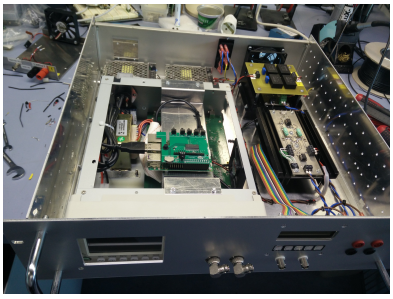

Figure 9.10: Complete assembly of the power standard

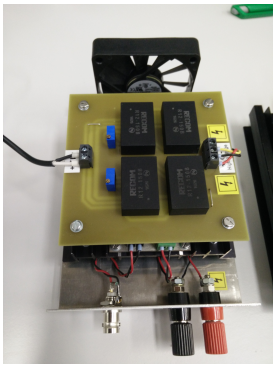

Figure 9.11: Assembled voltage amplifier

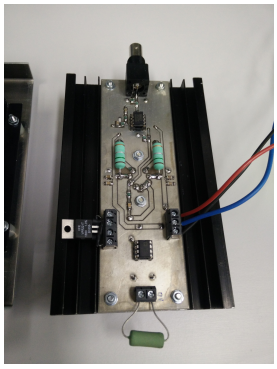

Figure 9.12: Assembled transconductance amplifier

(a) Starting

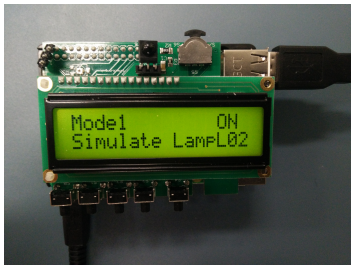

(b) Selecting

Figure 9.13: The user interface of Raspberry Pi when starting and selecting the waveform

The front panel of the dummy load device is shown in Figure 9.14. The screen (see "1" in Figure 9.14) displays waveforms and the buttons are used to select the next or the previous waveform, see "2". Totally there are 10 options: Sinusoidal, Harmonic, Simulate Lamp L01, L02, L04, L05, L06, L07, L08, L11. Use "on" or "off" to switch on or off the output of the signal generator which is fed to the transconductance amplifier and the voltage amplifier. The amplified current and voltage signals are output at I and U ports.

Figure 9.14: Front panel of the dummy load device. 1: waveform display screen. 2: button selecting screen. 3: I port. 4: U port.

9.5. MEASUREMENT RESULTS

THE input power variation of ten simulated lamps are measured and recorded in Table 9.3. It can be inferred from the results that the power variation of the dummy load device is very low, for example, 0.021 % variation can be achieved in the sinusoidal and harmonic simulation.

Table 9.3: Input power variation of ten simulated lamps

Lamp	Power variation
Sinusoidal	0.021 %
Harmonic	0.021 %
L01	0.243 %
L02	0.083 %
L04	0.068 %
L05	0.128 %
L06	0.153 %
L07	0.201 %
L08	0.158 %
L11	0.138 %

10

CONCLUSION

THE transfer standard designed in this project is a standard power reference source simulating the feature of SSL products that can achieve rapid stabilization, establish traceability of measurement results and generate consistent luminous flux for better light quality. This transfer standard can be applied as a common measurement tool to check the reliability of measurement setups in global test laboratories. The SSL products specifications accurately determined by precise measurement setups will increase consumer confidence in high-quality LED light bulbs and promote the energy-efficient LED technology to the lighting market.

The transfer standard driver consists of a constant power controller LM3447 and a linear regular LM317. The LM3447 uses primary side control and input voltage feedforward technique to control the input power. The LM317 is connected in series with the LED load and regulates the output current at a constant level.

Test on the transfer standard shows that the input power variation can be restricted to 0.21 % and the output current fluctuation can be limited to 0.24 % with the proposed topology as temperature rising. The results can be improved by using a series resistor with a low temperature coefficient for LM317, keeping the temperature on LM3447 board stable by fan, maintaining the LED temperature constant and so on.

Comparison between different measurement tools proves that the commercial LED lamp is not applicable in test laboratories because its input power variation of 3.66 % is quite large and it takes over 25 minutes to reach stabilization. With the transfer standard designed in this project, the 0.5 % demands of the standard scenario can be instantly achieved. Even though the input power variation of 1.63 % does not reach the aim of 0.1 % variation, the stabilization time for 0.1 % variation is only about 3.5 minutes, rather shorter than the 45 minutes for the commercial lamp.

As a result, the transfer standard using LM3447 and LM317 has a good performance of low power variation and rapid stabilization, which makes it reliable to behave as power reference for validating measurement setups in test laboratories.

On the other hand, the dummy load solution simulating the voltage and current characteristics of SSL produces is also able to establish traceability of measurement re-

sults and to provide highly accurate calibration for measurement setups. The bandwidth of the voltage amplifier is 200 kHz and the bandwidth of the transconductance amplifier is 100 kHz. Both upper frequencies can prevent distortion in the voltage and current waveforms. Measurement results show that the power variation of ten simulated LED lamps are all limited below 0.25 %. Therefore, the dummy load can regulate power better than the power electronics transfer standard.

Solid-state lighting (SSL) is the most energy-efficient lighting technology in the present lighting market. With high efficiency, good quality and nice lighting appearance, SSL products are highly expected to replace low efficient and environmental unfriendly incandescent light bulbs in the near future. An international organization has been established to develop harmonized regulations and global assessment scheme for SSL products. This project aims at designing a transfer standard to be used to check the reliability of measurement setups in test laboratories worldwide. Key features of the transfer standard are rapid stabilization and switchable configuration to simulate typical SSL topologies. The transfer standard is designed into two types of device: the first type is a power electronics converter using a constant-power controller, and the second type is a dummy load device simulating the voltage and current waveforms of SSL products. Those two types of transfer standards can both simulate the electrical characteristic of SSL products, achieve rapid stabilization and acquire reliable measurement results. Fluctuations and uncertainties in measurement are minimized. Compared to the commercial LED lamp, the transfer standard has smaller power variation and faster stabilization time, which make it applicable to check the reliability of measurement setups as power reference.